

IMPACT OF CLIMATE CHANGE ON DROUGHT IN ARAGON (NE SPAIN)

Emma Gaitán (1,2), Robert Monjo (2) Javier Pórtoles (2), María Rosa Pino-Otín (1)

(1) Universidad San Jorge. Villanueva de Gállego, 50830 Zaragoza, Spain.

(2) Fundación para la Investigación del Clima. C/ Tremps 11, 28040 Madrid, Spain.

- Emma Gaitán: emma@ficlima.org
- Robert Monjo: robert@ficlima.org
- Javier Pórtoles: javier@ficlima.org
- María Rosa Pino-Otín: rpino@usj.es (corresponding author)

Corresponding author:

María Rosa Pino-Otín. Universidad San Jorge. Campus Universitario Villanueva de Gállego
Autovía A-23 Zaragoza-Huesca, km. 510 50830 Villanueva de Gállego. Zaragoza (Spain).

T. 0034 976 060 100

M.0034 676 22 79 90

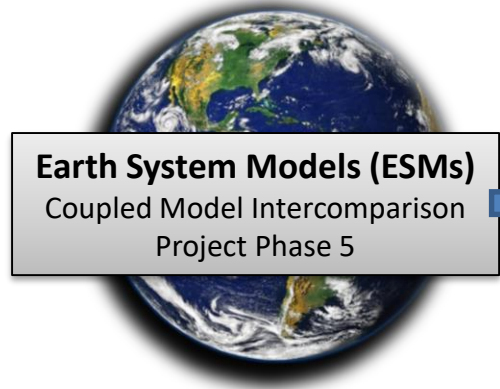
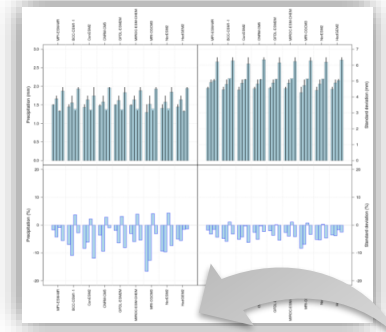
Fax. (34) 976 077 584

rpino@usj.es

www.usj.es

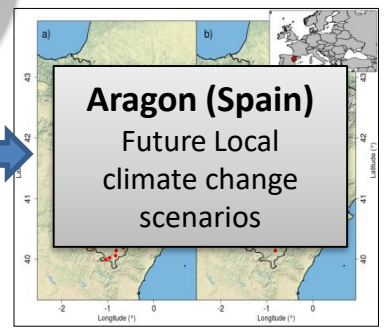
Validation

How accurately
ESMs simulate the
current climate
(precipitation)



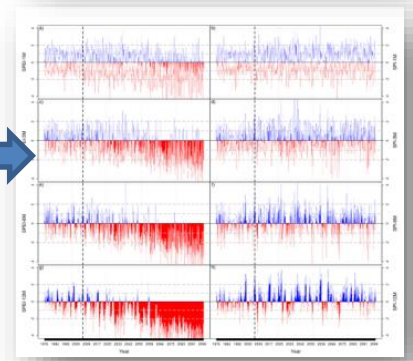
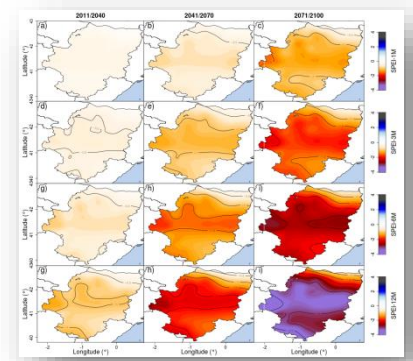
Earth System Models (ESMs)
Coupled Model Intercomparison
Project Phase 5

Downscaling
A two-step statistical
downscaling
methodology



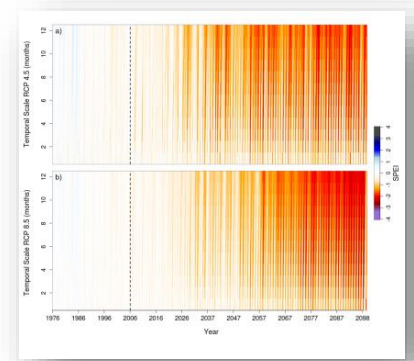
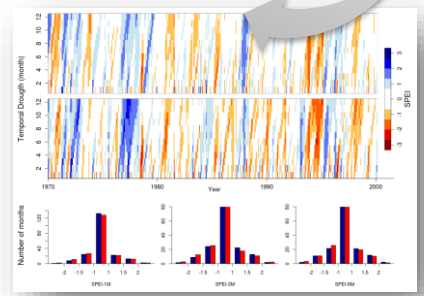
Aragon (Spain)
Future Local
climate change
scenarios

**Meteorological Drought
scenarios**



Verification

How
accurately the
downscaling methodology
simulates the current
climate (precipitation and
meteorological droughts
episodes)



Highlights:

- Future SPI and SPEI scenarios for Aragon (Spain) were downscaled.
- Scenarios were based on the most recent Earth System Models (CMPI5) at first time
- The SPI, considering only precipitation, shows no changes in the water balance.
- The SPEI, considering the global warming, shows an increase of the drought episodes
- Hydroclimatic conditions of Aragon will change towards a drier climate

1 Abstract

2 Droughts are one of the extreme climatic phenomena with the greatest and most
3 persistent impact on health, economic activities and ecosystems and are poorly
4 understood due to their complexity. The exacerbation of global warming throughout this
5 century probably will cause an increase in droughts, so accurate studies of future
6 projections at a local level, not done so far, are essential.

7 Climate change scenarios of drought indexes for the region of Aragon (Spain) based on
8 nine Earth System Models (ESMs) and two Representative Concentration Pathways
9 (RCPs) corresponding to the fifth phase of the Coupled Model Intercomparison Project
10 (CMIP5) have been generated for the first time. Meteorological Drought episodes were
11 analysed from three main aspects: magnitude (index values), duration and spatial
12 extent. The evolution of drought is also represented in a novel way, allowing
13 identification, simultaneously, of the intensity of the episodes as well as their duration in
14 different periods of accumulation and, for the first time, at the observatory level.

15 Future meteorological drought scenarios based on the Standardized Precipitation Index
16 (SPI) hardly show variations in water balance with respect to normal values. However,
17 the Standardized Precipitation Evapotranspiration Index (SPEI) which, in addition to
18 precipitation, considers evapotranspiration, shows a clear trend towards increasingly
19 intense periods of drought, especially when considering cumulative periods and those
20 at the end of the century.

21 Representation of the territory of the drought indexes reflects that the most populated
22 areas (Ebro Valley and SW of the region), will suffer the longest and most intense
23 drought episodes. These results are key in the development of specific measures for
24 adapting to climate change.

25 1. Introduction

26
27 Drought is probably one of the extreme climatic phenomena with the greatest impact
28 on the world's population and that can affect millions of people every year around the
29 planet (Bryant, 1991; Wilhite, 2000). It also has serious effects on the availability of
30 water and therefore on economic activities such as agriculture (Lesk et al., 2016) and
31 tourism and profound impacts on human health (Stanke et al., 2013) and ecosystems
32 (Alary et al., 2014) that may persist over time. (Dai, 2011). However, drought is a
33 phenomenon that is not well understood due to its complexity and lack of historical
34 records (Wilhite, 2000) and because it depends on numerous factors.

35 For this reason, the scientific community and institutions are putting a lot of effort into
36 understanding, identifying, documenting and monitoring this phenomenon more
37 exhaustively. Examples are the drought databases of the European Drought
38 Observatory, the National Drought Mitigation Center and, the historical database of the
39 Standardized Precipitation Evapotranspiration Index (SPEI)
40 (<http://spei.csic.es/database.html>).

41 1.1 Droughts types and indexes

42 Precipitation is the primary controlling factor of drought but other meteorological
43 phenomena, such as temperature (Cook et al., 2014; Hao et al., 2017; Livneh and
44 Hoerling, 2016), wind (McVicar et al., 2012a) and relative humidity (Willett et al., 2014),
45 can modulate its intensity (Bates et al., 2008). Through potential evapotranspiration
46 (PET), it is possible to evaluate the amount of water that would evaporate and transpire
47 if there was enough water available, which is very important in the evaluation of
48 meteorological droughts.

49 Because drought affects so many different aspects (environmental, economic, social,
50 health), a single 'drought' does not really exist. Drought is often classified into four
51 types (Wilhite, 2000; Wilhite et al., 1985): meteorological, agricultural, hydrological and
52 socioeconomic drought.

53 The main subject of the current study is meteorological drought, a type of drought
54 characterized by below-normal precipitation over a period of months to years and that
55 should be defined as a condition relative to the normal local condition (Dai, 2011;
56 Paparrizos et al.,2018; Wilhite, 2000).

57 On the other hand, to characterize droughts, standardized drought indexes are used in
58 the literature. These indexes are direct indicators based on climate information, defined
59 so that the results are comparable in time and space since droughts of the same
60 magnitude can have very different effects depending on the time of year and the place
61 where they occur (Hayes et al., 1999; Vicente-Serrano, 2016; Wilhite, 2000).

62 Some of these indexes are well established and have been used to monitor climatic
63 conditions across different locations; these include the Palmer Drought Severity Index
64 (PDSI; Palmer, 1965) and Standardized Precipitation Index (SPI; McKee et al., 1993),
65 for example. The Lincoln Declaration on Drought Indexes (Hayes et al., 2011)
66 determined that SPI is the only index, from the point of view of meteorological drought,
67 valid for any region of the world and any time scale, being one of the most used in
68 Europe (Spinoni et al., 2015). It is able to provide better spatial standardization than
69 PDSI (Lloyd-Hughes and Saunders, 2002) and indicate drought initiation and
70 termination because they are implicit parts of the index (Sonmez et al., 2005).

71 SPI, however, presents some limitations such as that it neglects the effect of
72 temperature increase and, therefore, the effect that an increase in PET (Vicente-
73 Serrano et al., 2010a) or in the atmospheric evaporative demand (AED) (Vicente-
74 Serrano et al, 2020) can have on droughts, which may affect prediction of the impact of
75 global warming in future drought conditions. It should be noted, however, that other
76 meteorological variables as wind speed, solar radiation and air humidity, can also affect
77 PET changes linked to climate change.

78 To avoid this problem, (Vicente-Serrano et al., 2010a) proposed a new climatic drought
79 index, SPEI, which considers the difference between monthly precipitation and AED.
80 Thus, SPEI best reflects climate change as it makes a more realistic measurement of

81 water availability by incorporating the effect of temperature on changes in evaporation
82 demand as does PDSI. On the other hand, it maintains the multi-temporal nature and
83 simplicity of SPI (Marcos-Garcia et al., 2017).

84 According to the latest report of the Intergovernmental Panel on Climate Change
85 (IPCC, 2014a), analysis of the precipitation regime (Calbo, 2010; Lavaysse et al.,
86 2012), droughts (Burke and Brown, 2008; Lopez-Bustins et al., 2013) and the extreme
87 temperatures that drastically increase evapotranspiration (ET) (Rebetez et al., 2006)
88 and decrease soil moisture (Sheffield and Wood, 2008) suggest that drought episodes
89 could become more severe around the world in the 21st century (Dai, 2013).

90 There are some studies that emphasize that future projections of drought may
91 overestimate drought episodes if future soil moisture (Berg et al., 2017) and runoff
92 (Yang et al., 2018) simulations are not taken into account (Berg and Sheffield, 2018),
93 which can affect AED. In addition, recent studies highlight the need to include CO₂
94 concentration in the analysis of AED under climate conditions since an increase of the
95 CO₂ acts contributing to the increase in temperatures that in turn affect the Vapour-
96 Pressure Deficit (VPD). On the other hand, CO₂ could increase water use efficiency by
97 plants reducing AED and therefore mitigate the drying (Dai et al., 2018; Roderick et al.,
98 2015).

99 In this context, most European areas and the Mediterranean region seem to be
100 prominent regional climate change hotspots where an increment in the occurrence of
101 extreme events is expected (Beniston et al., 2007; Skaugen et al., 2004). Specifically, a
102 possible rise in the intensity and frequency of extreme drought events is expected
103 (Forzieri et al., 2014; Hoerling et al., 2012; Iglesias et al., 2007; Marcos-Garcia et al.,
104 2017; Paparrizos et al., 2018), especially in the summer months (Vicente-Serrano et
105 al., 2010c), and will have significant environmental, social and economic impacts
106 (Blenkinsop and Fowler, 2007).

107 The global climate models used today reproduce temperature trends very well, but the
108 level of precision for large-scale precipitation patterns is lower than for temperature

109 (IPCC, 2014b). This has caused the climatic projections of droughts to show great
110 uncertainty and therefore we cannot know with precision the effects of climatic change
111 on drought severity at the regional level in the future (Burke and Brown, 2008). This is
112 especially problematic in areas with high precipitation variability, such as the
113 Mediterranean region, where the drought patterns derived from the results of global
114 climate models are not consistent (Vicente-Serrano et al., 2004).

115 1.2 Drought in NE Spain (Aragón)

116 In Spain, as in the rest of Europe (Feyen and Dankers, 2009), different series of major
117 droughts have been happening in recent decades. In addition, the literature seems to
118 indicate a trend towards an increase in meteorological water scarcity in the Iberian
119 Peninsula, either due to an increase in the frequency of drought episodes or due to a
120 change in the precipitation regime (Fragoso et al., 2018; Gallego et al., 2011; Garcia-
121 Barron et al., 2011; Machado et al., 2011; Ojeda et al., 2017; Vicente-Serrano et al.,
122 2004). This makes necessary studies at a local level and the development of future
123 scenarios of droughts which are adequate as possible for evaluating the local impacts
124 of climate change.

125 Drought scenarios in Spain are also scarce: either they are from studies conducted
126 prior to the Fifth Assessment Report of the United Nations Intergovernmental Panel on
127 Climate Change (IPCC5) and in very small areas (Lopez-Bustins et al., 2013) or they
128 use IPCC5 models but use dynamic downscaling information from the European
129 Coordinated Regional Downscaling Experiment (EUROCORDEX; (Collados-Lara et al.,
130 2018; Marcos-Garcia et al., 2017). The latter also evaluates only SPI and SPEI at the
131 12-month scale. However, these studies agree that the combined use of SPI and SPEI
132 is adequate for studying drought episodes in the future (Lopez-Bustins et al., 2013;
133 Marcos-Garcia et al., 2017).

134 The combined study of both indexes, SPEI and SPI could be an effective formula for an
135 adequate study of meteorological drought in territories with the climatology of Aragon
136 (NE Iberian Peninsula). This region of Spain is characterized by a continental

137 Mediterranean climate with high precipitation variability and marked by very diverse
138 orography throughout its territory that includes areas of high mountains, valleys and
139 steppes (López et al., 2007). In addition, we must consider that previous studies in
140 Aragon have shown that an increase in temperature is one of the variables that will be
141 most noticeable with climate change throughout this century (Gaitan et al., 2019;
142 Ribalaygua et al., 2013a).

143 As far as we know, drought scenarios in Aragon have not been obtained to date. As
144 has been seen, it is essential to have local scenarios to determine the impact of climate
145 change on the environmental or socioeconomic reality of each region in order to make
146 decisions on adaptation to climate change.

147 The goal of this study is to obtain, for the first time, meteorological drought scenarios
148 for Aragon (located in NE of Spain) for the 21st century using a statistical methodology
149 to downscale GCMs from CMIP5.

150 To achieve this goal, the capacity of the GCMs to simulate the past observed climate
151 was assessed (validation) and using CMIP5, precipitation scenarios for Aragon were
152 generated to simulate future daily precipitation.

153 Finally, as Aragon is a region sensitive to episodes of drought caused by a varying rate
154 of precipitation and high temperatures, the SPI and SPEI meteorological indexes were
155 calculated and the frequency of occurrence of drought and its spatial distribution were
156 simulated to identify the drought vulnerability of the study area. Drought indexes were
157 also verified.

158 This study provides, for the first time, scenarios of meteorological drought in the NE of
159 Spain according to CMIP5 models, useful for predicting the impacts of climate change
160 on the availability of water at a local scale and which are necessary for stakeholders to
161 make decisions on adaptation and mitigation of climate change. On the other hand, this
162 region of Spain is a good indicator of many characteristic areas of southern Europe
163 (high mountains, river basins, steppes, etc.).

164 2. Data and methodology

165 2.1. Study area

166 The present study was carried out in the region of Aragon (NE of Spain) (Fig. 1).
167 Because of its location, Aragon falls within the Western Mediterranean climate area
168 characterized by scarce precipitation with cool winters and hot, dry summers.
169 Differences in latitude between the most northern and most southern points of Aragon
170 (340 km length and 240 km width) along with the influence of the Cantabrian and
171 Mediterranean Seas and the general atmospheric circulation as well as the orographic
172 complexity of the region (extreme altitude differences of over 3000 m between the
173 plains (the Ebro River valley) and the mountains (the Pyrenees)), give rise to great
174 subclimate variety, with different thermal and pluviometric regimes that condition the
175 local climate (López et al., 2007).

176 Precipitation is scarce in most of Aragon and is distributed clearly according to relief, as
177 the isohyets are arranged in concentric circles decreasing from mountain areas to the
178 centre of the region. Although the average annual total precipitation of the Aragonese
179 territory is around 550 mm, there are regions for which the average is below these
180 values (for example, in the central sector of the Ebro Depression). Only in the
181 Pyrenees and, to a lesser extent, in the Iberian Mountain Range, does precipitation
182 reach important values, 1800–2000 mm, and show positive water balance values
183 (considering the difference between precipitation and AED). On the other hand, more
184 than 60% of the region has average values of AED above 1100 mm, showing a
185 negative water balance,

186 to which contributes not only the scarce rainfall but also the strong wind ("Cierzo")
187 characteristic of the Ebro Valley (López et al., 2007). Therefore, 70% of the Aragonese
188 territory is considered semi-arid (index value proposed by the United Nations
189 Environment Program < 0.5 and even 30% presents values of 0.3) (Cherlet et al.,
190 2018).

191 2.2. Datasets

192 2.2.1. Surface observation datasets

193 In this study, an observational dataset (daily maximum and minimum temperature and
194 precipitation) belonging to the extensive network of instrumental observatories owned
195 by the Spanish Meteorological Agency (AEMET) (<http://www.aemet.es>) was used (Fig.
196 1). This dataset is the same as the one used in previous studies (Gaitan et al., 2019;
197 Ribalaygua et al., 2013a) in order to work with a set of data that has been subjected to
198 strict quality control (inhomogeneities, gaps, outliers, transcription errors and so on)
199 carried out first by the Government of Aragon (López et al., 2007) and completed, in a
200 second phase, by (Ribalaygua et al., 2013a). As a complement to quality controls,
201 those stations with a large number of data gaps or less than 15 years of daily records
202 were discarded.

203 For the simulation of future climate scenarios of precipitation, a first set of 263 stations
204 was used (red dots in Fig. 1a). Of these 263 stations, just those with data for both
205 variables, temperature and precipitation, were used for the simulation of drought
206 indexes (43 stations, Fig. 1b).

207 2.2.2. Atmospheric dataset

208 A set of nine climate models were selected from CMIP5, supplied by the Program for
209 Climate Model Diagnosis and Intercomparison (PCMDI) archives.

210 The global climate models called Earth System Models (ESMs) from the fifth phase of
211 the Coupled Model Intercomparison Project (CMIP5) (Tripathi et al., 2006) have
212 contributed to the acquisition of both dynamic and statistical downscaling techniques
213 with less uncertainty. These models integrate the individual parts of the climate system
214 (atmosphere, ocean, land and sea ice) and the exchange of energy and mass between
215 them (Knutti and Sedlacek, 2013). These models also include chemical processes,
216 land use, plant and ocean ecology and an interactive carbon cycle, which enables
217 integration of biochemical processes into the models (Heavens et al., 2013),
218 constituting a robust set of coordinated climate model experiments (Carvalho et al.,
219 2017; Chen et al., 2016; Perez et al., 2014).

220 The climate models (Table 1) were selected according to the time resolution (daily) of
221 available predictor fields, because it is required for the downscaling method used. All of
222 the models were ESMs (Jones et al., 2011; Wang et al., 2009).

223 This study used data from two different experiment families of GCMs: the Historical
224 experiment (Taylor et al., 2012), which covers much of the industrial period and can be
225 referred to as 'twentieth-century' simulations, and the Representative Concentration
226 Pathway (RCP) family (Moss et al., 2010), which corresponds to different possible
227 ranges of radiative forcing reached in the year 2100 with respect to values of the pre-
228 industrial era. This study used future projections determined by the RCP8.5 'high'
229 scenario and RCP4.5 'intermediate' scenario, the core of IPCC5 experiments.

230 In order to study the behaviour of the CMIP5 model Historical simulations, we used the
231 reanalysis dataset from the European Centre for Medium-Range Weather Forecasts
232 (ECMWF ERA-40; <http://www.ecmwf.int/research/era/do/get/>) (Uppala et al., 2005) for
233 the period 1958–2000 at 6-hourly time resolution and 125 km spatial resolution. For
234 verification of the methodology, it was necessary to reduce the temporal and spatial
235 scale of the reanalysis in order to compare both ERA-40 and the climate model
236 simulations (Ribalaygua et al., 2013a; Ribalaygua et al., 2013b). The geographical
237 limits of the atmospheric window used were latitudes 31.5°N to 55.1°N and longitudes
238 27.0°W to 14.6°E, covering not only the geographic area under study but also the
239 surrounding atmosphere areas which exert a meteorological influence all over the
240 Iberian Peninsula (Ribalaygua et al., 2013a). The use of the ERA-40 data set has
241 allowed us to compare these new results with those published by Ribalaygua et al
242 2013a.

243 2.3. Methodologies

244 2.3.1. Validation and generation of future precipitation scenarios

245 A two-step analogue/regression statistical downscaling method developed previously
246 (Ribalaygua et al., 2013b) was applied to obtain future scenarios of precipitation and
247 drought. This method has been used in national and international projects, with good

248 verification results (Gaitan et al., 2019; Monjo et al., 2016; Moutahir et al., 2017;
249 Ribalaygua et al., 2018; Rodriguez et al., 2014; Santiago et al., 2017). This
250 methodology offers some advantages: it is computationally inexpensive, provides local
251 information and allows quantifying the uncertainty associated with the downscaling
252 process (Van der Linden and Mitchell, 2009). Other advantages are the application of
253 future simulations consistent with observations (physically coherent between them) and
254 using local scale (because nearby data points in space are not subjected to different
255 climate change conditions) (Ribalaygua et al., 2013b).

256 Through the validation process we can, on the one hand, evaluate the ability of each
257 ESM to simulate the predictor fields (comparing the downscaled Historical experiment
258 simulation for each model with the downscaled ERA-40 simulation for a common
259 period, 1958–2000) and, on the other, quantify the uncertainties inherent to future
260 climate projections through an ensemble strategy (Monjo et al., 2016).

261 Bias and standard deviation at seasonal scale have been used as error measures. This
262 validation process presents some limitations related to the observational data available
263 to be considered in the final uncertainty analysis. More information about the validation
264 process can be consulted in (Ribalaygua et al., 2013b).

265 Future local climate scenarios at local and daily scale for precipitation were produced
266 for nine ESMs (see Table 1) and two RCPs (RCP4.5 and RCP8.5) as a previous step
267 to calculate the drought indices. As precipitation is an essential variable in the analysis
268 of drought, these scenarios are a starting point providing initial information on future
269 pluviometric conditions.

270 The local climatic projections of precipitation belonging to CMIP5 were obtained in this
271 study using the same methodology as that used for temperature scenarios, previously
272 described (Gaitan et al., 2019).

273 *2.3.2. Drought indexes*

274 SPI was developed by McKee et al. (1993) and is based on two assumptions: 1) that
275 the variability of precipitation is greater than that of temperature and AED, and 2) that

276 the rest of the variables are stationary over time. The SPI value is defined as a
277 numerical value that represents the number of standard deviations of precipitation, over
278 the accumulation period in question, with respect to the average, once the original
279 distribution of precipitation has been transformed into a normal distribution (i.e., mean
280 of zero and standard deviation of 1). The SPI values can be interpreted as the number
281 of standard deviations by which the observed anomaly deviates from the long-term
282 mean.

283 SPEI developed by (Vicente-Serrano et al., 2010a) and revisited by (Begueria et al.,
284 2014) is a variant of the widespread SPI; it has greater potential as a drought index
285 since it considers the climate balance (through the difference between monthly
286 precipitation and AED). SPEI values can be interpreted in the same way as SPI values
287 (number of standard deviations by which the observed anomaly deviates from the long-
288 term mean).

289 Both indexes were calculated using the R package 'SPEI' (Version 1.7). The SPI was
290 calculated using Gamma distribution to fit the original precipitation series (Organization
291 WMO, 2012) and the SPEI was calculated using log-logistic distribution (Vicente-
292 Serrano et al., 2015; Vicente-Serrano and Beguería, 2016). The parameters of these
293 distributions were obtained by the method of unbiased probabilistic weighted moments
294 (Vicente-Serrano and Beguería, 2016). The scale of SPI and SPEI values used in the
295 study can be seen in Table 2.

296 The period 1976-2005 was used as a reference period, which represents the last 30
297 years of the Historical period. Based on this reference period, both the SPI and the
298 SPEI were calculated for the period 2006-2100. The choice of the reference period was
299 made to evaluate the future hydroclimatic conditions of the region with respect to the
300 average conditions of the last 30 years of the Historical experiment.

301 To obtain the AED values used in the calculation of SPEI, both the Hargreaves-Samani
302 (1985) and Thornthwaite (1948), formulas have been used, denominated SPEI-Har and
303 SPEI-Thor, respectively. These formulas were chosen to calculate AED because they

304 are recommended within the SPEI package and they also depend only on temperature
305 and precipitation, unlike other more complex methods such as the Penman–Monteith
306 (Smith M et al.,1998) and Jensen–Haise methods (Jensen and Haise, 1963). Both
307 methods only take into account the temperature, so it is assumed that the calculation of
308 AED trends could have certain limitations (Irmak et al., 2012b; McVicar et al., 2012b;
309 Sheffield et al., 2012). For a certain increase in the temperature, the change in the
310 obtained result can be higher than the one really expected according a complete
311 method like Penman-Monteith. Therefore, the role of AED on drought severity would be
312 overestimate and this would have some effect on the drought indices obtained for
313 future scenarios.

314 The way in which the indexes have been analysed follows the guidelines of the WMO
315 (WMO, 2017) which recommends analysis of a drought episode from three main
316 aspects – magnitude (index values), duration (alternation between positive and
317 negative values) and spatial extent – and all these aspects configure the severity of the
318 episode.

319 In order to assess the capacity of the downscaling methodology to simulate SPI and
320 SPEI, we analysed the intensity and duration of the different drought episodes shown
321 by both indexes, comparing the SPI and SPEI values calculated from the simulated
322 ERA-40 temperature and precipitation series with those obtained from the observed
323 series for a common period (1970-2000). Verification of the maximum and minimum
324 temperature and precipitation can be seen in a previous study (Ribalaygua et al.,
325 2013a). The statistical measures used in the verification processes were the bias,
326 standard deviation and Pearson correlation. The statistical measures were calculated
327 using R computing software (R Development Core Team, 2010).

328 From the ESM simulated temperature and precipitation series (nine ESMs and two
329 RCPs), we determined the drought episodes that are expected in Aragon during the
330 upcoming decades of the 21st century. The SPI and SPEI scenarios were compared to

331 a historical period (1976–2005) to analyse the future changes with respect to the actual
332 situation of these extreme events.

333 To draw future local climate scenario maps, we used Thin Plate Spline (TPS)
334 regression from the R package 'fields' (Nychka et al., 2015).

335

336 3. Results

337 3.1. Validation and precipitation scenarios

338 The results of the validation process (comparison between the ERA-40 precipitation
339 simulations and the historical precipitation simulations for each ESM for a common
340 period (1958–2000)) are shown in Fig. 2, for both absolute (mm) and relative
341 precipitation (%). The results are variable depending on the model and the seasonal
342 period; however, all the models are able to reproduce the annual cycle of precipitation
343 as well as the differences between seasonal periods (maximum values in autumn and
344 spring, followed by winter and summer). The obtained bias and standard deviation are
345 less than ± 1 mm/day, which in relative terms supposes a difference of less than or
346 around $\pm 10\%$ in the worst of the cases.

347 In general terms, a big variation in the Aragon precipitation regime is not expected.
348 According to scenario RCP8.5, mean variations in the amount of precipitation are
349 expected to be around $\pm 10\%$ for all seasons of the year, except for the summer where
350 no precipitation change is expected. Scenario RCP4.5 shows no precipitation
351 fluctuations throughout the 21st century with respect to current values (see support
352 information, Fig. S1 to S4).

353 3.2. Generation of future local climate scenarios of drought indexes

354 3.2.1. *Verification of drought index simulation*

355 To verify the simulation of drought indexes, the first step was to compare the SPI and
356 SPEI values obtained from the observations with those calculated from the simulated
357 series of ERA-40.

358 Fig. 3 shows the verification results corresponding to SPI at time scales from 1 month
359 (SPI-1M) to 12 months (SPI-12M) for the period 1970–2000 (Fig. 3a and 3b). This
360 process allows the identification of episodes of deficit or excess precipitation recorded
361 and simulated from ERA-40. In addition, the number of months in the period 1970–
362 2000 in which SPI values were obtained within different intensity ranges (Table 1) for
363 SPI-1M, SPI-3M and SPI-6M are shown (Fig. 3c, 3d and 3e).

364 As can be seen in Fig. 3a and 3b, the time series of the simulated SPI for ERA-40
365 shows, in an acceptable way, the same values presented by the observed SPI, with a
366 correlation of $p = 0.75$ in the case of SPI-1M, $p = 0.72$ for SPI- 3M, $p = 0.64$ for SPI-6M
367 and $p = 0.61$ for SPI-12M.

368 The simulated and observed SPI values show dry episodes (negative SPI) in similar
369 periods, for example the periods 1970–1972, 1978, 1981–1982, 1989, 1994–1995 and
370 1998. The same can be seen for wet episodes (positive SPI) as in, for example, the
371 periods 1976–1977, 1988 and 1996–1997.

372 Figs. 4 and S5 show the results of the verification process for SPEI based on SPEI-Har
373 and SPEI-Thor calculations, respectively.

374 Similar results were obtained for calculation of SPEI based on the Hargreaves method
375 (Fig. 4a and 4b) although in this case the correlation obtained between the observed
376 and simulated time series of SPEI is slightly higher (0.80 for SPEI-1M, 0.78 for SPEI-
377 3M, 0.72 for SPEI-6M and 0.73 for SPEI-12M).

378 When the Thornthwaite method is used for calculating AED in SPEI (see Fig. S5), the
379 temporal correlations are lower than those obtained with SPEI based on Hargreaves.

380 On the other hand, for about 65–70% of the period considered, water balance
381 conditions in Aragon was considered normal (SPI/SPEI between $-0,5$ and $0,5$),
382 suffering extreme wet or dry episodes for only 2–4% of the period 1970–2000.

383 The error (bias) made in the simulation of SPI (Fig. 3c to 3e) and SPEI (Fig. 4c to 4e) is
384 quite small for all of the classes considered ($< \pm 2$ months).

385 *3.2.2. Local climate scenarios to predict drought indexes*

386 Figs. 5 to 9 (complemented with Figs. S6 and S7) show the results obtained for the
387 simulation of SPI and SPEI throughout the 21st century from different perspectives.

388 Fig. 5 shows local climate change scenarios for future SPEI (a, c and d) and SPI (b, d
389 and f) at 3-, 6- and 12-month scale, which have been predicted on the basis of the nine
390 models (see Table 2) and here are used to obtain a general vision of the changes in
391 water balance for the Aragon region as a whole. The future projections of SPI and
392 SPEI for the period 2006-2100 have been made based on the reference period
393 (Historical 1976-2005). When working with normalized indexes, the future values of the
394 SPI and SPEI represent anomalies with respect to the average values of the reference
395 period, which allows to evaluate the future evolution of the hydric conditions in Aragon
396 with respect to the average of the last 30 years of the Historical experiment.

397 The SPI values obtained are hardly modified with respect to the Historical period so,
398 according to these results, the water balance characteristics of the region as a whole
399 would remain similar to the current ones. On the other hand, the SPEI climate change
400 scenarios, considering the effect of AED, show a marked tendency towards
401 increasingly negative values of the index with respect to the Historical period,
402 especially at the end of the century.

403 Both RCPs show a similar evolution until 2060, with changes of SPEI with respect to
404 the Historical period of -0.6 for SPEI-3M, -0.9 for SPEI-6M and -1.3 for SPEI-12M.
405 For the final period of the century, the variation begins to be more pronounced under
406 the conditions of RCP8.5, with changes of -1.2 for SPEI-3M, -1.8 for SPEI-6M and
407 -2.8 for SPEI-12M, while under scenario RCP4.5, SPEI values vary slightly from those
408 reached in 2060.

409 These results are very well reflected in the time-scale evolution maps, where the
410 simulated time series from 1976 to 2100 are represented, both for SPEI (Fig. 6) and
411 SPI (Fig. 7) and under both scenarios, RCP4.5 (Figs. 6a and 7a) and RCP8.5 (Figs. 6b
412 and 7b) with respect to different time scales (from 1 to 12 months).

413 Fig. 6 shows a tendency towards more and more extreme SPEI values, especially in
414 the longer time scales. For time scales of up to 4 months, an alternation between
415 periods considered normal and dry periods is expected (SPEI values between $-1,5$ and
416 $0,5$). For longer time scales, there is a tendency towards more intense and prolonged
417 periods of drought, with SPEI values of up to -3 at the end of the century. The pattern
418 obtained is similar under both RCPs, being more pronounced in the case of RCP8.5.
419 In the time-scale map corresponding to SPI (Fig. 7), the same pattern as that obtained
420 for SPEI is not appreciated; in this case, alternating dry and wet periods are observed
421 for all time scales, these being somewhat more extensive as we move along the time
422 scales. The same pattern is observed under both RCPs, the signal being slightly
423 stronger in the case of RCP8.5.

424 As a complement to the previous results, which allowed the extraction of results for the
425 water regime of Aragon as a whole, the spatial maps of both indexes are shown. Figs.
426 8 and 9 show the climate scenarios for mean SPEI according to RCP4.5 and RCP8.5,
427 respectively. These figures show the temporal evolution for four time scales: 1 month
428 (first row), 3 months (second row), 6 months (third row) and 12 months (fourth row).
429 The temporal periods chosen were 2011–2040 (present), 2041–2070 (mid-century) and
430 2071–2100 (end-century). Figs. S6 and S7 show the same information but for mean
431 SPI.

432 The results for SPEI vary considerably between different points in the Aragon region.
433 Coinciding with what was said before, it is observed how the SPEI values become
434 more extreme as the 21st century and time scales advance. The Ebro Valley area is
435 the one that will be subject to more intense episodes of precipitation shortage at the
436 end of the 21st century, with SPEI values from -1 at 3 months to -2 at 12 months
437 according to RCP4.5 and considerably more intense under RCP8.5 with values from
438 -1.8 at 3 months to -4 at 12 months. The north-west area of the region, which is
439 expected to be most affected by drought episodes, deserves special attention. The
440 Pyrenees zone is the one that will clearly suffer the fewest expected drought episodes;

441 under RCP4.5 it is expected to remain in normal water balance conditions while under
442 RCP8.5, at most, SPEI will reach values of -1.5 (at the end-century and at 12-month
443 time scale).

444 The SPI spatial maps (Figs. S6 and S7) show how the region will remain under normal
445 water balance conditions, highlighting the Ebro basin at the end of the 21st century and
446 under RCP8.5, where more negative values of SPI (around -1) are appreciated, but
447 which are still within the range considered normal for the region.

448 It is important to emphasize that if the average value of the SPEI/SPI tends to
449 increasingly negative values and if this is a constant trend in the future, the conditions
450 considered normal today will evolve towards new values considered normal (Vicente-
451 Serrano et al. 2020).

452 This study has been carried out for each of the observatories used in the study and for
453 each of the climatic models, which reveals that the entire region is going to be affected
454 by episodes of drought despite its location and height. As an example, the temporal
455 evolution of both indexes obtained according to the MPI-ESM-MR climate model and
456 under both RCPs is shown for the observatories of Zaragoza (Figs. 10 and 11) and
457 Cedrillas-Huesca (Figs. S8 and S9).

458 The choice of these observatories was based on the Climate Atlas of Aragon (López et
459 al., 2007), since they are two of the reference points used in the climatic
460 characterization of the region. The choice of these observatories was also made based
461 on their location; the Zaragoza observatory is located in the Zaragoza airport station at
462 a height of 263 m while the Cedrillas-Huesca observatory is located in the northern
463 area of the region at a height of 1347 m. In addition, the Zaragoza airport station is
464 considered representative of the variability of temperatures in Aragon (Roldan et al.,
465 2011).

466 The expected temporal evolution of SPEI throughout the 21st century is consistent with
467 that explained above, but as it is a single climatic model and uses a single observatory,
468 the alternation between wet and dry periods can be seen more clearly at a time scale

469 of 1 to 3 months. Also, as we move forward in the time scales, this alternation softens,
470 resulting in periods of more intense and prolonged precipitation shortage while, for SPI,
471 the alternation between wet and dry periods is observed for all time scales. This
472 highlights, as for SPI, how periods with positive SPI for the Cedrillas-Huesca
473 observatory are more intense and prolonged than those predicted for Zaragoza.

474

475 4. Discussion

476 These results offer the possibility of having future climate projections based on recently
477 updated data, allowing the evaluation of how drought could affect the region of Aragon,
478 both spatially and temporarily, and can be taken as a reference to analyse its impact on
479 multiple sectors. Temporally, drought increases to the end of the century; at the
480 territory level, the area most affected will be the central area of the Ebro Valley, where
481 most of the population in the area is concentrated.

482 The difficulty of developing impact studies and quantifying their damage as a result of
483 periods of water scarcity comes mainly from the lack of observed values and studies at
484 a local level with future projections, hence the need to publish studies of these
485 characteristics.

486 In this study, climate change scenarios of drought indexes for the region of Aragon,
487 Spain, based on nine ESMs corresponding to CMIP5 have been generated for the first
488 time.

489 The evolution of two indexes, SPI and SPEI, has been obtained throughout this century
490 and also over the territory, which has allowed us to observe that while SPI, which only
491 considers precipitation, shows few changes, SPEI, that considers temperature and
492 incorporates the effects of AED, shows a tendency towards periods of increasingly
493 intense drought, especially when considering accumulated periods of longer duration
494 and those at the end of the century. Therefore, in the current climate change context it
495 is essential to take into account the effect of temperature in the study of droughts.

496 Figs. 6 and 7 represent a novel representation of the evolution of drought, allowing
497 identification, simultaneously, of the intensity of the episodes and their duration in
498 different periods of accumulation.

499 One of the strengths of this study is the use of local climate scenarios (at the
500 observatory level) to generate future drought indexes. Having this information will
501 facilitate decision-making in the face of expected changes based on what is expected
502 to occur at each observatory and not in the region a whole. As an example of the study
503 at local level, the results of future climate scenarios for Zaragoza (representative
504 observatory of Aragon, Roldan et al., 2011) and Cedrillas-Huesca (support information)
505 are shown.

506 4.1. Precipitation scenarios used for the simulation of drought indexes.

507 For the simulation of precipitation, ESMs have been used instead of climatic models.
508 ESMs are the most powerful climatic models to date and incorporate significant
509 improvements (Flato et al., 2014) that allow better accuracy in climate simulation, as
510 can be seen in the good results obtained in the validation process.

511 Validation of the ESMs has shown good results for simulating precipitation. Both the
512 obtained bias and standard deviation are less than ± 1 mm/day, which in relative terms
513 supposes differences of less than or around $\pm 10\%$ in the worst cases; however, those
514 values are within the order of natural variability of precipitation. These results are better
515 than those obtained for the generation of scenarios of the fourth IPCC report published
516 by (Ribalaygua et al., 2013a) particularly in the summer months, a particularly critical
517 time in Aragon.

518 The results obtained for the processes of verification of the methodology (Ribalaygua
519 et al., 2013a) and validation of the ESMs are good enough to allow the use of local
520 climatic scenarios generated under these conditions in impact studies and analysis of
521 extreme episodes such as periods of precipitation shortage.

522 Future precipitation scenarios show, under RCP8.5 conditions, a slight decrease in
523 precipitation throughout the 21st century for all seasons of the year, except for the

524 summer months where there is hardly any variation compared to current values of
525 precipitation in the region. Under RCP4.5 conditions, less pessimistic than the previous
526 one, barely any precipitation changes are expected at any time of the year.

527 These results are consistent with those published by AEMET (www.aemet.es) and
528 directly by the IPCC (Mukherjee et al., 2018), although the latter show the direct
529 outputs of the ESMs and do not carry the added value of applying downscaling
530 techniques.

531 4.2. Consideration of the simulation of drought indexes

532 SPI is considered by experts in this field as one of the few indexes applicable in any
533 region of the world for any time scale (Hayes et al., 2011) and with multiple advantages
534 of application compared to other indexes of widespread use such as PDSI (Dracup et
535 al., 1980; Guttman, 1998; Hayes et al., 2011; Hayes et al., 1999; Vicente-Serrano et
536 al., 2010b). In the context of climate change with significant temperature variations
537 (Gaitan et al., 2019), SPEI has been chosen; its formulation is similar to that of SPI and
538 allows the comparison of both indexes and evaluation of the future behaviour of
539 drought episodes considering the effects of future temperature changes. Both indexes
540 have been verified and used previously in Aragon (Vicente-Serrano et al., 2010a). We
541 have only used the temperature in the calculation of AED because the absence of
542 observed historical data of variables such as radiation or humidity does not allow us a
543 correct validation process of certain indices such as Penman that include these
544 variables.

545 4.2.1. Verification results

546 In general, the results of the verification process show good correlations between the
547 observed and simulated time series for both indexes for the period 1970–2000, higher
548 ones being obtained for SPEI. This is consistent with the results published by Vicente-
549 Serrano et al. (2012); they obtained higher correlations for the calculation of SPEI than
550 SPI, especially for the summer months, which are the most critical in the region of
551 Aragon.

552 The temporal series based on observations are satisfactorily represented by the
553 temporal series based on simulations, recreating almost all dry and wet episodes of
554 importance. It is observed how both the simulated SPI and SPEI tend, for the majority
555 of times, to present dry and humid periods of greater intensity than those observed,
556 especially for longer time scales, as occurred in 1976–1977 for positive values of the
557 indexes and in 1981–1982 for negative ones. In general, the number of months of the
558 period 1970–2000 located within each of the classes defined for SPI/SPEI has been
559 simulated very satisfactorily.

560 The dry and wet periods detected in this study coincide with or are approximate to
561 those published previously (Vicente-Serrano and Lopez-Moreno, 2005) based on SPI
562 (dry episodes: 1986–1987, 1989 and 1994–1997; wet episodes: 1976–1980), in the
563 Climate Atlas of Aragon (López et al., 2007) based on the precipitation regime (dry
564 episodes: 1970, 1985, 1993 and 1995), by Spinoni (Spinoni et al., 2015) based on a
565 combined 12-month index (dry episodes: 1979–1980 and 1995–1998) and by
566 Tselepidaki (Tselepidaki et al., 1992) from a European study (dry episode: 1989),
567 among others. In some cases, the years are not exactly the same because of the use
568 of different drought and temporal scale indexes.

569 *4.2.2. Future scenarios*

570 The uncertainties associated with both processes, verification and validation, should be
571 considered when interpreting future scenarios. For drought projections the focus should
572 be on changes in the frequency and magnitude of cases located at the lower tail of the
573 distribution as was recommended by Vicente-Serrano et al. (2019).

574 Future meteorological drought scenarios based on SPI barely show water balance
575 variations with respect to normal values, regardless of the time scale considered and
576 the region of Aragon, except for the Ebro Valley where there is a slight sign of drought
577 at the end of the 21st century and under the conditions of RCP8.5.

578 These results were expected due to precipitation scenarios barely showing changes
579 throughout the 21st century.

580 When considering other climatic variables, such as temperature, the drought scenarios
581 based on SPEI show a clear trend towards increasingly dry periods and longer
582 droughts, especially in the Ebro area and south-west of the region. According to the
583 trends shown by the temperature and precipitation scenarios obtained for Aragon, the
584 results obtained were expected. The fact that the results obtained at the 12-month
585 scale are more intense than those of 1-3 months is partly a result of the way in which
586 drought indices are formulated and the autoregressive component of its metric so that
587 when the timescale increases, changes in the frequency of drought conditions increase
588 more in comparison to changes in the mean state. Although, recently, Vicente-Serrano
589 et al (2019) showed that these changes are independent of the metric with which these
590 indices have been calculated, changes in the frequency of drought conditions increase
591 more in comparison to changes in the mean state.

592 The lack of consideration of variables such as temperature, wind or humidity in the
593 calculation of SPI means that this index presents certain limitations under global
594 warming conditions(Mishra and Singh, 2010; Mishra and Singh, 2011; Vicente-Serrano
595 et al., 2010a) and it is for this reason that, when considering AED in the calculation of
596 SPEI, such different results are obtained, especially at the end of the century and not
597 only under the conditions of RCP8.5, that some authors consider less realistic
598 (Hausfather and Peters, 2020), but also of RCP4.5.

599 Some studies recommend the use of PET and add value against global warming (Hu
600 and Willson, 2000; Vicente-Serrano et al., 2010a),Tsakiris and Vangelis, 2005). Recent
601 studies (Vicente-Serrano et al. 2019; Vicente-Serrano et al., 2020) suggest using AED
602 in the future study of droughts, as well as analyzing the impact caused by the increase
603 in CO₂ (Yang et al., 2019). Probably, considering the response that vegetation could
604 have to an increase in CO₂ and, therefore, in the evapotranspiration process, could
605 provide some variation in the future evolution of drought episodes that should be
606 explored in future studies.

607 The results of future drought scenarios presented here show results in line with those
608 obtained in other studies where it is concluded that the Mediterranean regions will
609 experience an increase in the severity and frequency of droughts (Stagge et al., 2015)
610 as a result of a slight decrease in precipitation and an abrupt increase in temperatures
611 (European Environment Agency, 2010; (Stagge et al., 2015) and which represent an
612 increase in water scarcity (Estrela et al., 2012). More specifically in the region of
613 Aragon, the ECCE project, based on dynamic downscaling and scenarios of the fourth
614 IPCC report (Ministerio de Medio Ambiente, 2011), showed a future decline of the
615 Ebro runoff, and Cook (Cook et al., 2014), based on scenarios of the fifth IPCC report
616 but without downscaling, obtained an increase in drought episodes based on SPEI.

617 *4.2.3. Impact on the territory*

618 Although there have been studies on the Aragon area, none present as complete a
619 picture as this study, combining drought evaluation with SPI and SPEI (that is,
620 considering the effect of global warming) based on scenarios of the fifth IPCC report
621 and providing the added value of working at the local scale by applying a downscaling
622 technique.

623 The scenarios obtained in this study indicate that the Ebro Valley, the most populated
624 area in the region that includes the largest city, Zaragoza with more than 650.000
625 people, will be most susceptible to future periods of extreme drought and will suffer
626 periods of drought of greater intensity and duration, especially at the end of this
627 century, which will have consequences in sectors such as health, water management,
628 economy and society in general (Lee et al., 2017).

629 It is remarkable that, in previous publications (Ribalaygua et al., 2013a), we detected
630 that the highest values of maximum temperature, especially at the end of the century
631 and in summer (around 40 °C) as well as the greatest intensity of heatwaves will also
632 take place in this area, so it will be especially vulnerable and these data should be
633 considered in the development of specific measures for adapting to climate change.

634 Adaptation to climate change in each region requires studies applied to the climatic
635 dynamics of each territory, so downscaling quality studies are essential for this.
636 However, these results at the local level are also useful for the whole of the southern
637 Iberian Peninsula and central Europe, since Aragon brings together geographical and
638 climatic features representative also of these other areas.

639

640 5. Conclusions

641 The generation for the first time of climate change scenarios of drought indexes for the
642 region of Aragon (Spain) based on nine ESMS and two RCPs from CMIP5 has allowed
643 us to obtain simultaneously the most accurate representation to date of the magnitude,
644 duration and intensity of meteorological drought episodes and their duration in different
645 periods of accumulation in this area of Spain. The use of different drought indices and
646 drought time-scales and its graphic representation is a relevant novelty in the scientific
647 literature.

648 This has allowed the detection of a clear trend towards increasingly intense periods of
649 drought, especially at the end of the century when cumulative periods of longer
650 duration are considered. This trend is detected only in the future drought scenarios
651 based on SPEI (which in addition to precipitation, considers AED), while in the SPI-
652 based scenarios it is softened. These results reinforce the need to study these extreme
653 phenomena in a context of climate change, considering the temperature.

654 At the territory level, spatial representation allowed us to discover that the area that will
655 be most affected by longer and more intense periods of drought, but also the greatest
656 decrease in precipitation (around 10%), is the Ebro Valley, the area that concentrates
657 most of the population as well as the main economic activities of the zone. The results
658 have also allowed, for the first time, the study of future drought indexes at the
659 observatory level, specifically for the most populous city, Zaragoza.

660 To cope effectively with the impacts of these extreme events that are expected in the
661 present century, it is essential to be able to generate local scenarios that accurately

662 describe climate change at the territory level. On the one hand, our results not only
663 confirm a trend already described in the Mediterranean area of an increase in the
664 severity and frequency of droughts but can also serve as a model and sentinel for
665 similar areas, since it has very varied climatic and orographic conditions.

666

667 REFERENCES

668

669 Alary V, Messad S, Aboul-Naga A, Osman MA, Daoud I, Bonnet P, et al. Livelihood strategies
670 and the role of livestock in the processes of adaptation to drought in the Coastal Zone
671 of Western Desert (Egypt). *Agricultural Systems* 2014; 128: 44-54.

672 Bates B, Kundzewicz Z, Wu S, Palutikof J. *Climate Change and water*. 2008. Eds. IPCC
673 Secretariat, Geneva, 210 pp

674 Begueria S, Vicente-Serrano SM, Reig F, Latorre B. Standardized precipitation
675 evapotranspiration index (SPEI) revisited: parameter fitting, evapotranspiration
676 models, tools, datasets and drought monitoring. *International Journal of Climatology*
677 2014; 34: 3001-3023.

678 Beniston M, Stephenson DB, Christensen OB, Ferro CAT, Frei C, Goyette S, et al. Future
679 extreme events in European climate: an exploration of regional climate model
680 projections. *Climatic Change* 2007; 81: 71-95.

681 Bentsen M, Bethke I, Debernard JB, Iversen T, Kirkevåg A, Seland O, et al. The Norwegian Earth
682 System Model, NorESM1-M - Part 1: Description and basic evaluation of the physical
683 climate. *Geoscientific Model Development* 2013; 6: 687-720.

684 Berg A, Sheffield J. *Climate Change and Drought: the Soil Moisture Perspective*. *Current*
685 *Climate Change Reports* 2018; 4: 180-191.

686 Berg A, Sheffield J, Milly PCD. Divergent surface and total soil moisture projections under
687 global warming. *Geophysical Research Letters* 2017; 44: 236-244.

688 Blenkinsop S, Fowler HJ. Changes in European drought characteristics projected by the
689 PRUDENCE regional climate models. *International Journal of Climatology* 2007; 27:
690 1595-1610.

691 Breshears D. An ecologist's perspective of ecohydrology, *Bull. Ecol. Soc. Am.*, 2005; 86: 296 –
692 300.

693 Bryant. EA. *Natural hazards*. *International Journal of Climatology*, E. Cambridge University
694 Press, Cambridge. ISBN 0 521 37295 X. 1993; 13:344-346.
695 <https://doi.org/10.1002/joc.3370130310>

696 Burke EJ, Brown SJ. Evaluating uncertainties in the projection of future drought. *Journal of*
697 *Hydrometeorology* 2008; 9: 292-299.

698 Calbo J. Possible Climate Change Scenarios with Specific Reference to Mediterranean Regions.
699 In: Sabater S, Barcelo D, editors. *Water Scarcity in the Mediterranean: Perspectives*
700 *under Global Change*. 8, 2010, pp. 1-13.

701 Carvalho D, Rocha A, Gomez-Gesteira M, Santos CS. Potential impacts of climate change on
702 European wind energy resource under the CMIP5 future climate projections.
703 *Renewable Energy* 2017; 101: 29-40.

704 Chen YD, Li JF, Zhang Q. Changes in site-scale temperature extremes over China during 2071-
705 2100 in CMIP5 simulations. *Journal of Geophysical Research-Atmospheres* 2016; 121:
706 2732-2749.

707 Cherlet M, Hutchinson C, Reynolds J, Hill J, Sommer S, von Maltitz G. (Eds.), *World Atlas of*
708 *Desertification*, Publication Office of the European Union, Luxembourg, 2018. United
709 Nations Environment Program

710 Chylek P, Li J, Dubey M, Wang M, Lesins G. Observed and model simulated 20th century Arctic
711 temperature variability: Canadian Earth System Model CanESM2. *Atmos. Chem. Phys.*
712 *Discuss.* 2011; 11: 22893–22907. <https://doi.org/10.5194/acpd-11-22893-2011>

713

714 Collados-Lara AJ, Pulido-Velazquez D, Pardo-Iguzquiza E. An Integrated Statistical Method to
715 Generate Potential Future Climate Scenarios to Analyse Droughts. *Water* 2018; 10.

716 Collins W, Bellouin N, Doutriaux-Boucher M, Gedney N, Hinton T, Jones CD, Liddicoat S, Martin
717 G, O'Connor F, Rae J, Senior C, Totterdell I, Woodward S, Reichler T, Kim J, Halloran P.

718 2008. Evaluation of the HadGEM2 model. Hadley Centre Technical Note. HCTN 74, Met
719 Office Hadley Centre, Exeter, UK.

720 Cook BI, Smerdon JE, Seager R, Coats S. Global warming and 21st century drying. *Climate*
721 *Dynamics* 2014; 43: 2607-2627.

722 Dai, A. G., T. B. Zhao, and J. Chen. 2018. "Climate Change and Drought: A Precipitation and
723 Evaporation Perspective." *Current Climate Change Reports* 4, no. 3 (Sep): 301-312.
724 <http://dx.doi.org/10.1007/s40641-018-0101-6>.

725 Dai AG. Drought under global warming: a review. *Wiley Interdisciplinary Reviews-Climate*
726 *Change* 2011; 2: 45-65.

727 Dai AG. Increasing drought under global warming in observations and models (vol 3, pg 52,
728 2013). *Nature Climate Change* 2013; 3: 171-171.

729 Dracup JA, Lee KS, Paulson EG. ON THE STATISTICAL CHARACTERISTICS OF DROUGHT EVENTS.
730 *Water Resources Research* 1980; 16: 289-296.

731 Estrela T, Perez-Martin MA, Vargas E. Impacts of climate change on water resources in Spain.
732 *Hydrological Sciences Journal-Journal Des Sciences Hydrologiques* 2012; 57: 1154-
733 1167.

734 Feyen L, Dankers R. Impact of global warming on streamflow drought in Europe. *Journal of*
735 *Geophysical Research-Atmospheres* 2009; 114.

736 Flato G, Marotzke J, Abiodun B, Braconnot P, Chou SC, Collins W, et al. Evaluation of Climate
737 Models, 2014.

738 Forzieri G, Feyen L, Rojas R, Florke M, Wimmer F, Bianchi A. Ensemble projections of future
739 streamflow droughts in Europe. *Hydrology and Earth System Sciences* 2014; 18: 85-
740 108.

741 Fragoso M, Carraca MD, Alcoforado MJ. Droughts in Portugal in the 18th century: A study
742 based on newly found documentary data. *International Journal of Climatology* 2018;
743 38: 5522-5541.

744 Gaitan E, Monjo R, Portoles J, Pino-Otin MR. Projection of temperatures and heat and cold
745 waves for Aragon (Spain) using a two-step statistical downscaling of CMIP5 model
746 outputs. *Science of the Total Environment* 2019; 650: 2778-2795.

747 Gallego MC, Trigo RM, Vaquero JM, Brunet M, Garcia JA, Sigro J, et al. Trends in frequency
748 indices of daily precipitation over the Iberian Peninsula during the last century. *Journal*
749 *of Geophysical Research-Atmospheres* 2011; 116.

750 Garcia-Barron L, Aguilar M, Sousa A. Evolution of annual rainfall irregularity in the southwest of
751 the Iberian Peninsula. *Theoretical and Applied Climatology* 2011; 103: 13-26.

752 Guttman NB. Comparing the Palmer Drought Index and the standardized precipitation index.
753 *Journal of the American Water Resources Association* 1998; 34: 113-121.

754 Hao ZC, Hao FH, Singh VP, Ouyang W. Quantitative risk assessment of the effects of drought on
755 extreme temperature in eastern China. *Journal of Geophysical Research-Atmospheres*
756 2017; 122: 9050-9059.

757 Hargreaves GL, Samani ZA. 1985. Reference crop evapotranspiration from temperature. *Appl.*
758 *Eng. Agric.* 1985;1: 96-99.

759 Hausfather Z, Peters GP. Emissions - the 'business as usual' story is misleading. *Nature* 2020;
760 577: 618-620.

761 Hayes M, Svoboda M, Wall N, Widhalm M. The lincoln declaration on drought indices. *Bulletin*
762 *of the American Meteorological Society* 2011; 92: 485-488.

763 Hayes MJ, Svoboda MD, Wilhite DA, Vanyarkho OV. Monitoring the 1996 drought using the
764 standardized precipitation index. *Bulletin of the American Meteorological Society*
765 1999; 80: 429-438.

766 Heavens N, Ward D, Natalie M. Studying and projecting climate change with earth System
767 Models. *Nat. Educ. Knowl.* 2013; 4 (5): 4.

768 Hoerling M, Eischeid J, Perlwitz J, Quan XW, Zhang T, Pegion P. On the Increased Frequency of
769 Mediterranean Drought. *Journal of Climate* 2012; 25: 2146-2161.

770 Hu Q, Willson GD. Effects of temperature anomalies on the Palmer Drought Severity Index in
771 the central United States. *International Journal of Climatology* 2000; 20: 1899-1911.

772 Iglesias A, Garrote L, Flores F, Moneo M. Challenges to manage the risk of water scarcity and
773 climate change in the Mediterranean. *Water Resources Management* 2007; 21: 775-
774 788.

775 IPCC, 2014a. *Climate Change 2014: Impacts, Adaptation, and Vulnerability. Part A: Global and*
776 *Sectoral Aspects. Contribution of Working Group II to the Fifth Assessment Report of*
777 *the Intergovernmental Panel on Climate Change.* Cambridge University Press,
778 Cambridge, United Kingdom and New York, NY, USA, p. 1132

779 IPCC, 2013. Stocker T, Qin D, Plattner G-K, Tignor M, Allen S, Boschung J, Nauels A, Xia Y, Bex V,
780 Midgley P (eds) *Climate Change 2013: the Physical Science Basis. Contribution of*
781 *Working Group I to the Fifth Assessment Report of the Intergovernmental Panel on*
782 *Climate Change.* Cambridge University Press, Cambridge.
783 doi:10.1017/CBO9781107415324

784 Irmak S, Kabenge I, Skaggs KE, Mutiibwa D. Trend and magnitude of changes in climate
785 variables and reference evapotranspiration over 116-yr period in the Platte River
786 Basin, central Nebraska-USA. *Journal of Hydrology* 2012b; 420: 228-244.

787 Iversen T, Bentsen M, Bethke I, Debernard JB, Kirkevag A, Seland O, et al. The Norwegian Earth
788 System Model, NorESM1-M - Part 2: Climate response and scenario projections.
789 *Geoscientific Model Development* 2013; 6: 389-415.

790 Jensen M and Haise H. Estimating Evapotranspiration from Solar Radiation. *Journal*
791 *Jones CD, Hughes JK, Bellouin N, Hardiman SC, Jones GS, Knight J, et al. The HadGEM2-ES*
792 *implementation of CMIP5 centennial simulations. Geoscientific Model Development*
793 *2011; 4: 543-570.*

794 Knutti R, Sedlacek J. Robustness and uncertainties in the new CMIP5 climate model
795 projections. *Nature Climate Change* 2013; 3: 369-373.

796 Lavaysse C, Vrac M, Drobinski P, Lengaigne M, Vischel T. Statistical downscaling of the French
797 Mediterranean climate: assessment for present and projection in an anthropogenic
798 scenario. *Natural Hazards and Earth System Sciences* 2012; 12: 651-670.

799 Lee SH, Yoo SH, Choi JY, Bae S. Assessment of the Impact of Climate Change on Drought
800 Characteristics in the Hwanghae Plain, North Korea Using Time Series SPI and SPEI:
801 1981-2100. *Water* 2017; 9.

802 Lesk C, Rowhani P, Ramankutty N. Influence of extreme weather disasters on global crop
803 production. *Nature* 2016; 529: 84-+.

804 Livneh B, Hoerling MP. The Physics of Drought in the US Central Great Plains. *Journal of*
805 *Climate* 2016; 29: 6783-6804.

806 Lloyd-Hughes B, Saunders MA. A drought climatology for Europe. *International Journal of*
807 *Climatology* 2002; 22: 1571-1592.

808 Lopez-Bustins JA, Pascual D, Pla E, Retana J. Future variability of droughts in three
809 Mediterranean catchments. *Natural Hazards* 2013; 69: 1405-1421.

810 López F, Cabrera M, Cuadrat JM. *Atlas Climático de Aragón.* First ed. Spain: J. Factory; 2007.

811 Machado MJ, Benito G, Barriendos M, Rodrigo FS. 500 Years of rainfall variability and extreme
812 hydrological events in southeastern Spain drylands. *Journal of Arid Environments*
813 *2011; 75: 1244-1253.*

814 Marcos-García P, Lopez-Nicolas A, Pulido-Velazquez M. Combined use of relative drought
815 indices to analyze climate change impact on meteorological and hydrological droughts
816 in a Mediterranean basin. *Journal of Hydrology* 2017; 554: 292-305.

817 Marsland SJ, Haak H, Jungclaus JH, Latif M, Roske F. The Max-Planck-Institute global ocean/sea
818 ice model with orthogonal curvilinear coordinates. *Ocean Modelling* 2003; 5: 91-127.

819 McVicar TR, Roderick ML, Donohue RJ, Li LT, Van Niel TG, Thomas A, et al. Global review and
820 synthesis of trends in observed terrestrial near-surface wind speeds: Implications for
821 evaporation. *Journal of Hydrology* 2012a; 416: 182-205.

822 McVicar TR, Roderick ML, Donohue RJ, Van Niel TG. Less bluster ahead? Ecohydrological
823 implications of global trends of terrestrial near-surface wind speeds. *Ecohydrology*
824 2012b; 5: 381-388.

825 Mckee T, Doesken N and Kleist J. The Relationship of Drought Frequency and Duration Times
826 Scales. American Meteorological Society. 8th Conference on Applied Climatology.
827 1993: January 17–22 Anaheim, California, pp. 179–184.

828 Ministerio de Medio Ambiente, 2005. Assessment report of the preliminary impacts in Spain
829 due to Climate Change. Centro de publicaciones del Ministerio de Medio Ambiente,
830 Madrid.

831 Mishra AK, Singh VP. A review of drought concepts. *Journal of Hydrology* 2010; 391: 204-216.

832 Mishra AK, Singh VP. Drought modeling - A review. *Journal of Hydrology* 2011; 403: 157-175.

833 Monjo R, Gaitan E, Portoles J, Ribalaygua J, Torres L. Changes in extreme precipitation over
834 Spain using statistical downscaling of CMIP5 projections. *International Journal of*
835 *Climatology* 2016; 36: 757-769.

836 Moss RH, Edmonds JA, Hibbard KA, Manning MR, Rose SK, van Vuuren DP, et al. The next
837 generation of scenarios for climate change research and assessment. *Nature* 2010;
838 463: 747-756.

839 Moutahir H, Bellot P, Monjo R, Bellot J, Garcia M, Touhami I. Likely effects of climate change
840 on groundwater availability in a Mediterranean region of Southeastern Spain.
841 *Hydrological Processes* 2017; 31: 161-176.

842 Mukherjee S, Mishra A, Trenberth KE. Climate Change and Drought: a Perspective on Drought
843 Indices. *Current Climate Change Reports* 2018; 4: 145-163.

844 Nychka D, Furrer R, Paige J, Sain S, 2015. *Fields: tools for spatial data*. R package version 9.0.
845 (URL: <http://doi.org/10.5065/D6W957CT>). www.image.ucar.edu/fields.

846 Organization WMO. (2012) In: Svoboda, M., Hayes, M. and Wood, D.(Eds.) *Standardized Precipitation*
847 *Index User Guide*. Geneva: WMO.

848 Ojeda MG, Gamiz-Fortis SR, Castro-Diez Y, Esteban-Parra MJ. Evaluation of WRF capability to
849 detect dry and wet periods in Spain using drought indices. *Journal of Geophysical*
850 *Research-Atmospheres* 2017; 122: 1569-1594.

851 Palmer W. «Meteorological Drought». Research paper no.45, U.S. Department of Commerce
852 Weather Bureau, febrero de 1965 (58 páginas). Available in National Climatic Data
853 Center de NOAA: [http://www.ncdc.noaa.gov/temp-and-](http://www.ncdc.noaa.gov/temp-and-precip/drought/docs/palmer.pdf)
854 [precip/drought/docs/palmer.pdf](http://www.ncdc.noaa.gov/temp-and-precip/drought/docs/palmer.pdf)

855 Paparrizos S, Maris F, Weiler M, Matzarakis A. Analysis and mapping of present and future
856 drought conditions over Greek areas with different climate conditions. *Theoretical and*
857 *Applied Climatology* 2018; 131: 259-270.

858 Perez J, Menendez M, Mendez FJ, Losada IJ. Evaluating the performance of CMIP3 and CMIP5
859 global climate models over the north-east Atlantic region. *Climate Dynamics* 2014; 43:
860 2663-2680.

861 Raddatz TJ, Reick CH, Knorr W, Kattge J, Roeckner E, Schnur R, et al. Will the tropical land
862 biosphere dominate the climate-carbon cycle feedback during the twenty-first
863 century? *Climate Dynamics* 2007; 29: 565-574.

864 R Development Core Team, 2010. *R: A Language and Environment for Statistical Comput-ing*. R
865 Foundation for Statistical Computing, Vienna, Austria 3-900051-07-0 [http://www.R-](http://www.R-project.org)
866 [project.org](http://www.R-project.org), Accessed date: 6 July 2011.

867 Rebetz M, Mayer H, Dupont O, Schindler D, Gartner K, Kropp JP, et al. Heat and drought 2003
868 in Europe: a climate synthesis. *Annals of Forest Science* 2006; 63: 569-577.

869 Ribalaygua J, Gaitan E, Portoles J, Monjo R. Climatic change on the Gulf of Fonseca (Central
870 America) using two-step statistical downscaling of CMIP5 model outputs. *Theoretical*
871 *and Applied Climatology* 2018; 132: 867-883.

872 Ribalaygua J, Rosa Pino M, Portoles J, Roldan E, Gaitan E, Chinarro D, et al. Climate change
873 scenarios for temperature and precipitation in Aragon (Spain). *Science of the Total*
874 *Environment* 2013a; 463: 1015-1030.

875 Ribalaygua J, Torres L, Portoles J, Monjo R, Gaitan E, Pino MR. Description and validation of a
876 two-step analogue/regression downscaling method. *Theoretical and Applied*
877 *Climatology* 2013b; 114: 253-269.

878 Roderick, M. L., P. Greve, and G. D. Farquhar. 2015. "On the Assessment of Aridity with
879 Changes in Atmospheric Co2." *Water Resources Research* 51, no. 7 (Jul): 5450-5463.
880 <http://dx.doi.org/10.1002/2015wr017031>.

881 Rodriguez R, Navarro X, Casas MC, Ribalaygua J, Russo B, Pouget L, et al. Influence of climate
882 change on IDF curves for the metropolitan area of Barcelona (Spain). *International*
883 *Journal of Climatology* 2014; 34: 643-654.

884 Roldán E, Gómez M, Pino-Otín R, Esteban M, Díaz, J. Determinación de zonas isotérmicas y
885 selección de estaciones meteorológicas representativas en Aragón como base para la
886 estimación del impacto del cambio climático sobre la posible relación entre mortalidad
887 y temperatura. *Rev Esp Salud Pública* 2011; 85: 457-469

888 Santiago JM, Munoz-Mas R, Solana-Gutierrez J, de Jalon DG, Alonso C, Martinez-Capel F, et al.
889 Waning habitats due to climate change: the effects of changes in streamflow and
890 temperature at the rear edge of the distribution of a cold-water fish. *Hydrology and*
891 *Earth System Sciences* 2017; 21.

892 Sheffield J, Wood EF, Roderick ML. Little change in global drought over the past 60 years.
893 *Nature* 2012; 491: 435-+.

894 Sheffield J, Wood EF. Projected changes in drought occurrence under future global warming
895 from multi-model, multi-scenario, IPCC AR4 simulations. *Climate Dynamics* 2008; 31:
896 79-105.

897 Skaugen T, Astrup M, Roald LA, Forland E. Scenarios of extreme daily precipitation for Norway
898 under climate change. *Nordic Hydrology* 2004; 35: 1-13.

899 Smith M, Allen R, Pereira L. Revised FAO methodology for crop-water requirements.
900 Management of nutrients and water in rainfed arid and semi-arid areas. Proceedings
901 of a consultants meeting. International Atomic Energy Agency (IAEA). 1998; IAEA-
902 TECDOC--1026. Ref. number: 29062763.

903 Sonmez FK, Komuscu AU, Erkan A, Turgu E. An analysis of spatial and temporal dimension of
904 drought vulnerability in Turkey using the standardized precipitation index. *Natural*
905 *Hazards* 2005; 35: 243-264.

906 Spinoni J, Naumann G, Vogt JV, Barbosa P. The biggest drought events in Europe from 1950 to
907 2012. *Journal of Hydrology-Regional Studies* 2015; 3: 509-524.

908 Stagge JH, Kohn I, Tallaksen LM, Stahl K. Modeling drought impact occurrence based on
909 meteorological drought indices in Europe. *Journal of Hydrology* 2015; 530: 37-50.

910 Stanke C, Kerac M, Prudhomme C, Medlock J, Murray V. Health effects of drought: a
911 systematic review of the evidence. *PLoS Curr.* 2013 Jun 5;5: pii:
912 ecurrents.dis.7a2cee9e980f91ad7697b570bcc4b004.
913 DOI: 10.1371/currents.dis.7a2cee9e980f91ad7697b570bcc4b004.

914 Taylor KE, Stouffer RJ, Meehl GA. AN OVERVIEW OF CMIP5 AND THE EXPERIMENT DESIGN.
915 *Bulletin of the American Meteorological Society* 2012; 93: 485-498.

916 Thornthwaite C. An approach toward a rational classification of climate. *Geogr. Rev.*1948; 38:
917 55–94.

918 Tripathi S, Srinivas VV, Nanjundiah RS. Downscaling of precipitation for climate change
919 scenarios: A support vector machine approach. *Journal of Hydrology* 2006; 330: 621-
920 640.

921 Tsakiris, G., and Vangelis, H. 2005. Establishing a drought index incorporating
922 evapotranspiration. *European Water* 2005; 9 (10): 3–11.

923 Tselepidaki I, Zarifis B, Asimakopoulos DN. LOW PRECIPITATION OVER GREECE DURING 1989-
924 1990. *Theoretical and Applied Climatology* 1992; 46: 115-121.

925 Uppala SM, Kallberg PW, Simmons AJ, Andrae U, Bechtold VD, Fiorino M, et al. The ERA-40 re-
926 analysis. *Quarterly Journal of the Royal Meteorological Society* 2005; 131: 2961-3012.

927 Van der Linden P and Mitchell, J (eds.): ENSEMBLES: Climate Change and its Impacts. Summary
928 of research and results from the ENSEMBLES project. Met Office Hadley Centre,
929 FitzRoy Road, Exeter EX1 3PB, UK. 160pp (2009).

930 Vicente-Serrano SM, McVicar TR, Miralles DG, Yang YT, Tomas-Burguera M. Unraveling the
931 influence of atmospheric evaporative demand on drought and its response to climate
932 change. *Wiley Interdisciplinary Reviews-Climate Change* 2020; 11.

933 Vicente-Serrano SM, Dominguez-Castro F, McVicar TR, Tomas-Burguera M, Pena-Gallardo M,
934 Noguera I, et al. Global characterization of hydrological and meteorological droughts
935 under future climate change: The importance of timescales, vegetation-CO2 feedbacks
936 and changes to distribution functions. *International Journal of Climatology*. 2019.
937 <https://doi.org/10.1002/joc.6350>

938 Vicente-Serrano SM, Begueria S. Comment on 'Candidate distributions for climatological
939 drought indices (SPI and SPEI)' by James H. Stagge et al. *International Journal of*
940 *Climatology* 2016; 36: 2120-2131.

941 Vicente-Serrano SM. FOREWORD: DROUGHT COMPLEXITY AND ASSESSMENT UNDER CLIMATE
942 CHANGE CONDITIONS. *Cuadernos De Investigacion Geografica* 2016; 42: 7-11.

943 Vicente-Serrano SM, Van der Schrier G, Begueria S, Azorin-Molina C, Lopez-Moreno JI.
944 Contribution of precipitation and reference evapotranspiration to drought indices
945 under different climates. *Journal of Hydrology* 2015; 526: 42-54.

946 Vicente-Serrano, S.M. Spatial and temporal evolution of precipitation droughts in Spain in the
947 last century in *Adverse Weather in Spain*; Martínez, C.C.-L.; Rodríguez, F.V., Eds.; WCRP
948 Spanish Committee: Madrid, Spain, 2013; 283–296.

949 Vicente-Serrano SM, Begueria S, Lopez-Moreno JI. A Multiscalar Drought Index Sensitive to
950 Global Warming: The Standardized Precipitation Evapotranspiration Index. *Journal of*
951 *Climate* 2010a; 23: 1696-1718.

952 Vicente-Serrano SM, Begueria S, Lopez-Moreno JI, Angulo M, El Kenawy A. A New Global 0.5
953 degrees Gridded Dataset (1901-2006) of a Multiscalar Drought Index: Comparison with
954 Current Drought Index Datasets Based on the Palmer Drought Severity Index. *Journal*
955 *of Hydrometeorology* 2010b; 11: 1033-1043.

956 Vicente-Serrano SM, Gonzalez-Hidalgo JC, de Luis M, Raventos J. Drought patterns in the
957 Mediterranean area: the Valencia region (eastern Spain). *Climate Research* 2004; 26:
958 5-15.

959 Vicente-Serrano SM, Lasanta T, Gracia C. Aridification determines changes in forest growth in
960 *Pinus halepensis* forests under semiarid Mediterranean climate conditions. *Agricultural*
961 *and Forest Meteorology* 2010c; 150: 614-628.

962 Vicente-Serrano SM, Lopez-Moreno JI. Hydrological response to different time scales of
963 climatological drought: an evaluation of the Standardized Precipitation Index in a
964 mountainous Mediterranean basin. *Hydrology and Earth System Sciences* 2005; 9: 523-
965 533.

966 Voltaire A, Sanchez-Gomez E, Melia DSY, Decharme B, Cassou C, Senesi S, et al. The CNRM-
967 CM5.1 global climate model: description and basic evaluation. *Climate Dynamics* 2013;
968 40: 2091-2121.

969 Wang B, Zhou TJ, Yu YQ. A View of Earth System Model Development. *Acta Meteorologica*
970 *Sinica* 2009; 23: 1-17.

971 Watanabe S, Hajima T, Sudo K, Nagashima T, Takemura T, Okajima H, et al. MIROC-ESM 2010:
972 model description and basic results of CMIP5-20c3m experiments. *Geoscientific Model*
973 *Development* 2011; 4: 845-872.

974 Wilhite D. Drought as a natural hazard: concepts and definitions. In: Wilhite DA, ed. *Droughts:*
975 *Global Assessment*. London: Routledge; 2000; 3–18.

976 Wilhite, D.A., Glantz, M.H. (1985). Understanding the drought phenomenon: The role of
977 definitions. *Water International* 10(3): 111-120

978 Willett KM, Dunn RJH, Thorne PW, Bell S, de Podesta M, Parker DE, et al. HadISDH land surface
979 multi-variable humidity and temperature record for climate monitoring. *Climate of the*
980 *Past* 2014; 10: 1983-2006.

981 WMO (World Meteorological Organization), 2017. Statement on the State of the Global
982 Climate in 2016. Nº 1189.2017. ISBN 978-92-63-11189-0

983 Xiao-Ge X, Tong-Wen W, Jie Z. Introduction of CMIP5 experiments carried out with the climate
984 system models of Beijing Climate Center. *Adv. Clim. Chang. Res.* 2013; 4:41–49.
985 <https://doi.org/10.3724/SP.J.1248.2013.041>

986 Yang YT, Roderick ML, Zhang SL, McVicar TR, Donohue RJ. Hydrologic implications of
987 vegetation response to elevated CO2 in climate projections. *Nature Climate Change*
988 2019; 9: 44-+.

989 Yang YT, Zhang SL, McVicar TR, Beck HE, Zhang YQ, Liu B. Disconnection Between Trends of
990 Atmospheric Drying and Continental Runoff. *Water Resources Research* 2018; 54:
991 4700-4713.

992 Yukimoto S, Yoshimura H, Hosaka M, Sakami T, Tsujino H, Hirabara M, Tanaka T, Deushi M,
993 Obata A, Nakano H, Adachi Y, Shindo E, Yabu S, Ose T, Kitoh A. 2011. Meteorological
994 research institute- earth system model v1 (MRI-ESM1)— model description. Technical
995 Report of MRI. vol 64.

996

GFDL-ESM2M	2°x2,5° daily	<u>National Oceanic and Atmospheric Administration</u> (NOAA), E.E.U.U.	Dunne et al. (2012)
CanESM2	2,8°x2,8° daily	Canadian Centre for Climate Modeling and Analysis (CC-CMA), Canadá.	Chylek et al. (2011)
CNRM-CM5	1,4°x1,4° daily	CNRM (Centre National de Recherches Meteorologiques), Meteo-France, Francia.	Voltaire et al. (2013)
BCC-CSM1-1	1,4°x1,4° daily	Beijing Climate Center (BCC), China Meteorological Administration, China.	Xiao-Ge et al. (2013)
HADGEM2-CC	1,87°x1,25° daily	Met Office Hadley Center, United Kingdom.	Collins et al. (2008)
MIROC-ESM-CHEM	2,8°x2,8° daily	Japan Agency for marine-Earth Science and Technology (JAMSTEC), Atmosphere and Ocean Research Institute (AORI), and National Institute for Environmental Studies (NIES), Japan.	Watanabe et al. (2011)
MPI-ESM-MR	1,8°x1,8° daily	Max-Planck Institute for Meteorology (MPI-M), Germany.	Raddatz et al. (2007); Marsland et al. (2003)
MRI-CGCM3	1,2°x1,2° daily	Meteorological Research Institute (MRI), Japan.	Yukimoto et al. (2011)
NorESM1-M	2,5°x1,9° daily	Norwegian Climate Centre (NCC), Norway.	Bentsen et al. (2012); Iversen et al. (2013)

Table 1. Information about the nine climate models belonged to the 5 Coupled Model Intercomparison Project (CMIP5) corresponding to the fifth report of the IPCC. Models were supplied by the Program for Climate Model Diagnosis and Intercomparison (PCMDI) archives.

SPEI/SPI	
≥ 2	extremely wet
1.5 a 2	severely wet
0.5 a 1.5	moderately wet
-0.5 a 0.5	normal values
$-1.5 \leq -0.5$	moderately dry
$-1.5 \leq -2$	severely dry
≤ -2	extremely dry

Table 2. SPEI/SPI Intensities Scale (Vicente-Serrano et al 2010a)

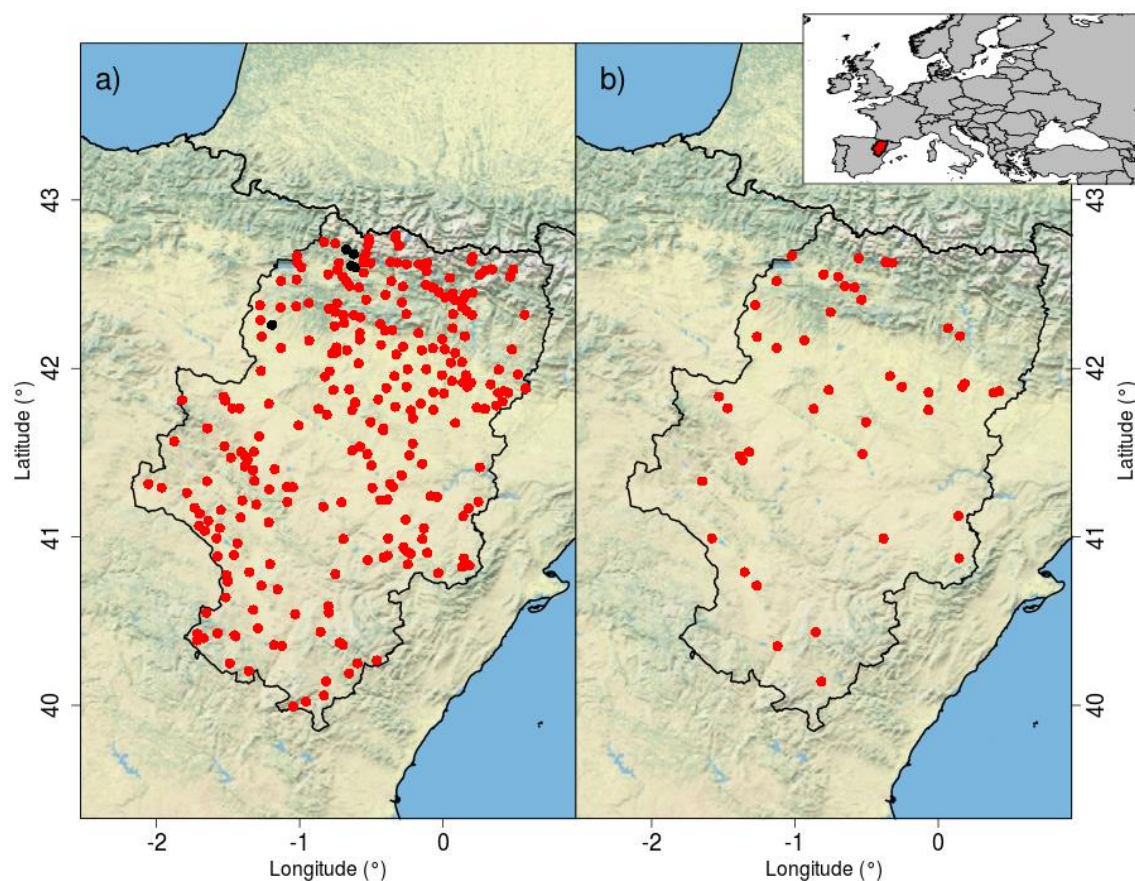


Figure 1. Location of the study Area and observatories. Aragon (Spain) in Europe. Points indicate the stations used in the study. a) Stations of precipitation (264) used in the generation of climate regional scenarios of precipitation (verification, validation and scenarios). b) Stations used exclusively on the generation of drought indexes (43). Map source: OpenStreetMap.

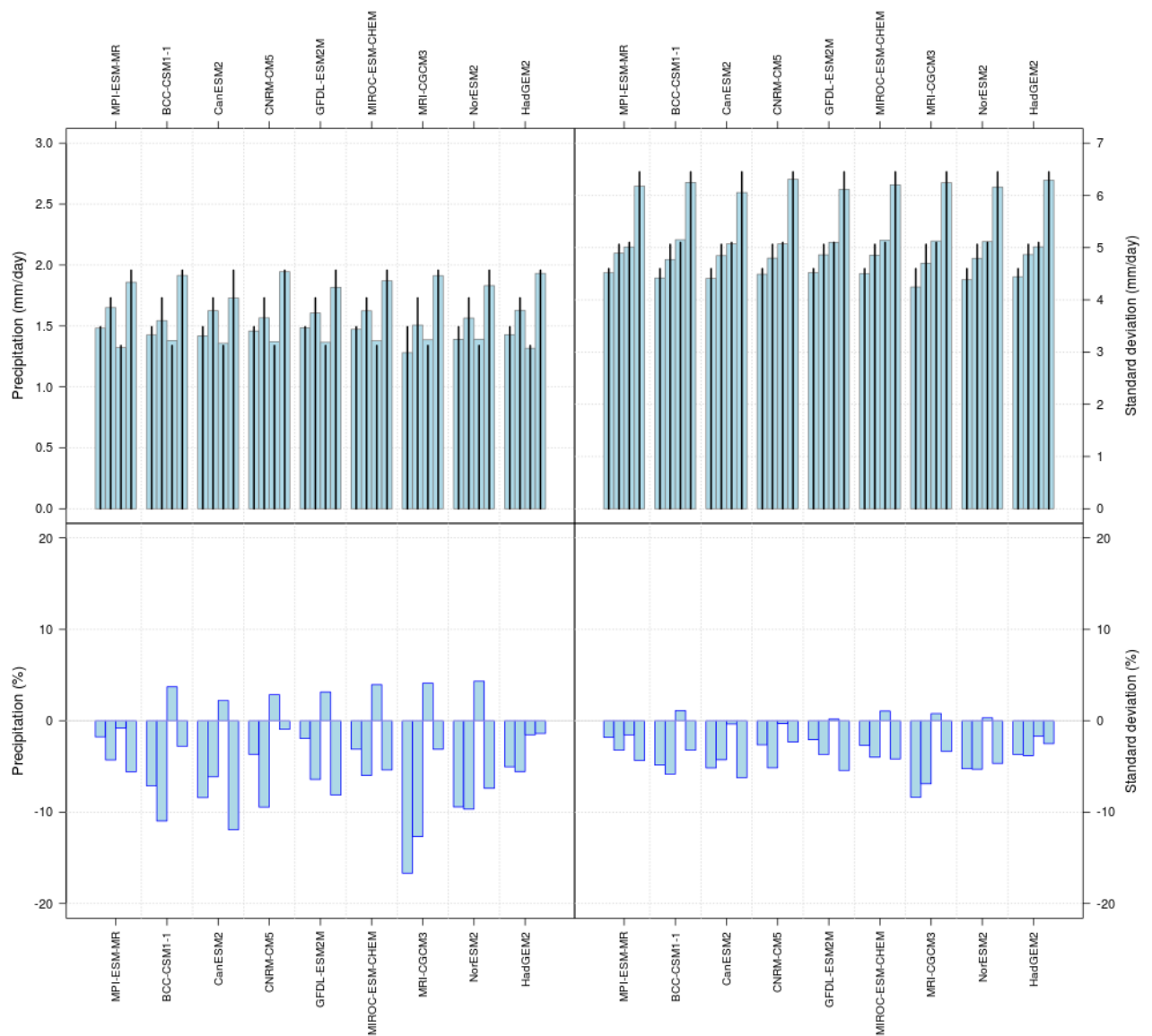


Figure 2. Validation of precipitation. Comparison between the precipitations obtained using the downscaled Historical data of the global climate models and the downscaled reanalysis data, for every seasonal period. Two graphs at the top: seasonal comparative between the precipitation simulated using the downscaled Historical data (colour bars) and that of the downscaled reanalysis data (black lines) for each global climate models (see Table 1) and for the four seasons: winter (December-February; first bar of each group of four), spring (March-May, second bar), summer (June-August; third bar) and autumn (September-November; four bar).

Two graphs at the bottom: relative seasonal differences between the simulated data using the downscaled Historical data and that of the downscaled reanalysis data.

Seasonal precipitation amounts are shown on the left columns and seasonal values of the standard deviation on the right columns.

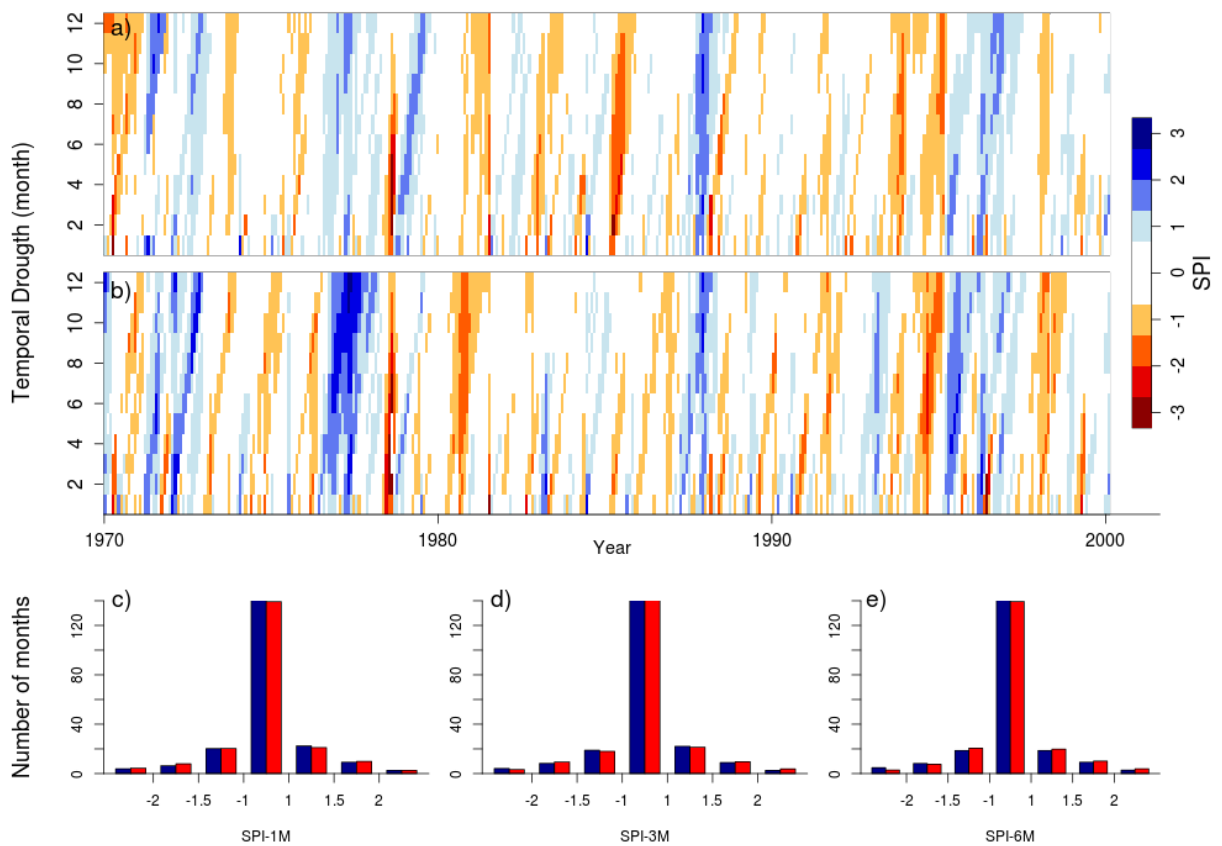


Figure 3. SPI verification. Results of the verification process for the SPI. a) time series of the SPI index calculated from observed data at the time-scales from 1 to 12 months for the period 1970-2000, b) time series of the SPI index calculated from downscaled ERA-40 at the time-scales from 1 to 12 months for the period 1970-2000. c), d) and e) number of months within the 1970-2000 period corresponding to each interval of the SPI intensities scale based on observed data (blue columns) and on downscaled ERA-40 (red columns) for the time-scales of 1, 3 and 6 months. Average of the all the stations used in the simulations.

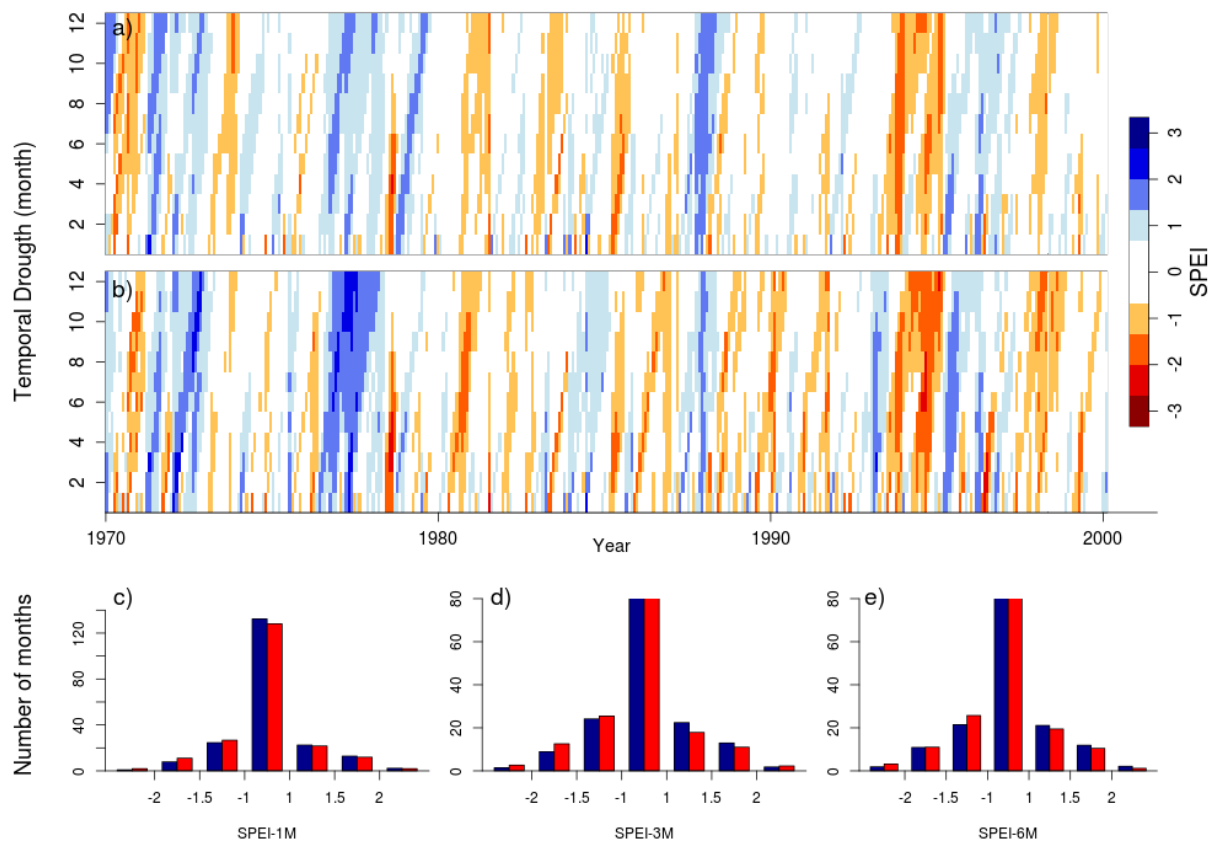


Figure 4. SPEI Har verification. Results of the verification process for the SPEI based on Hargraves Evapotranspiration. a) time series of the SPEI index calculated from observed data at the time-scales from 1 to 12 months for the period 1970-2000, b) time series of the SPEI index calculated from downscaled ERA-40 at the time-scales from 1 to 12 months for the period 1970-2000. c), d) and e) number of months within the 1970-2000 period corresponding to each interval of the SPI intensities scale based on observed data (blue columns) and on downscaled ERA-40 (red columns) for the time-scales of 1, 3 and 6 months. Average of the all the stations used in the simulations.

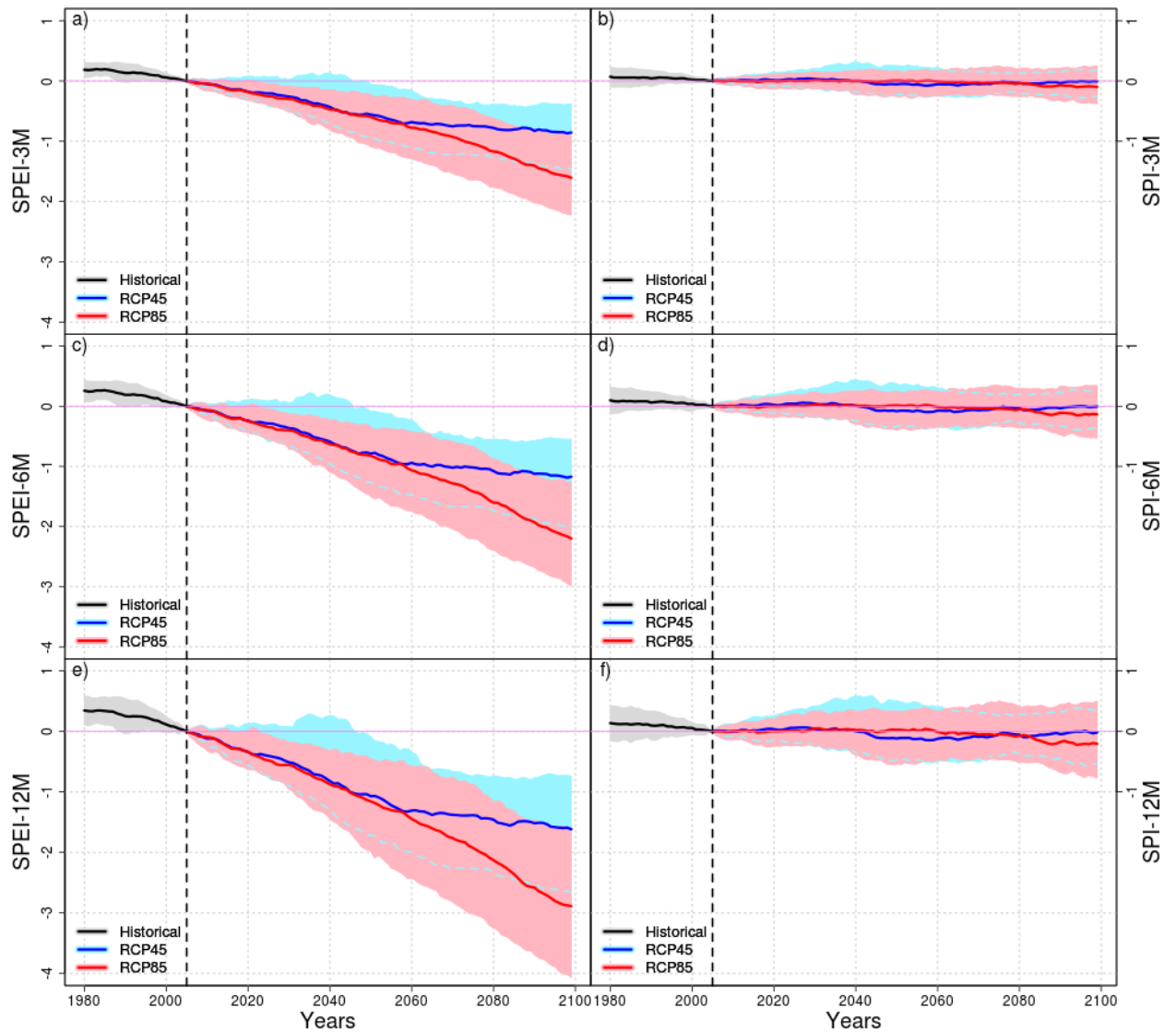


Figure 5. Simulated SPEI and SPI for the twenty-first century. Values are displayed as absolute increase compared to the amount simulated for the 1976–2005 Historical period for the time scales 3 months (a and b), 6 months (c and d) and 12 months (e and f). The vertical dotted line marks the end of the Historical data (2005). Data grouped for every RCP simulation of every global climate model selected and for the last 30 years of every station. The ensemble median (solid lines) and the 10th–90th percentile (shaded areas) values are displayed.

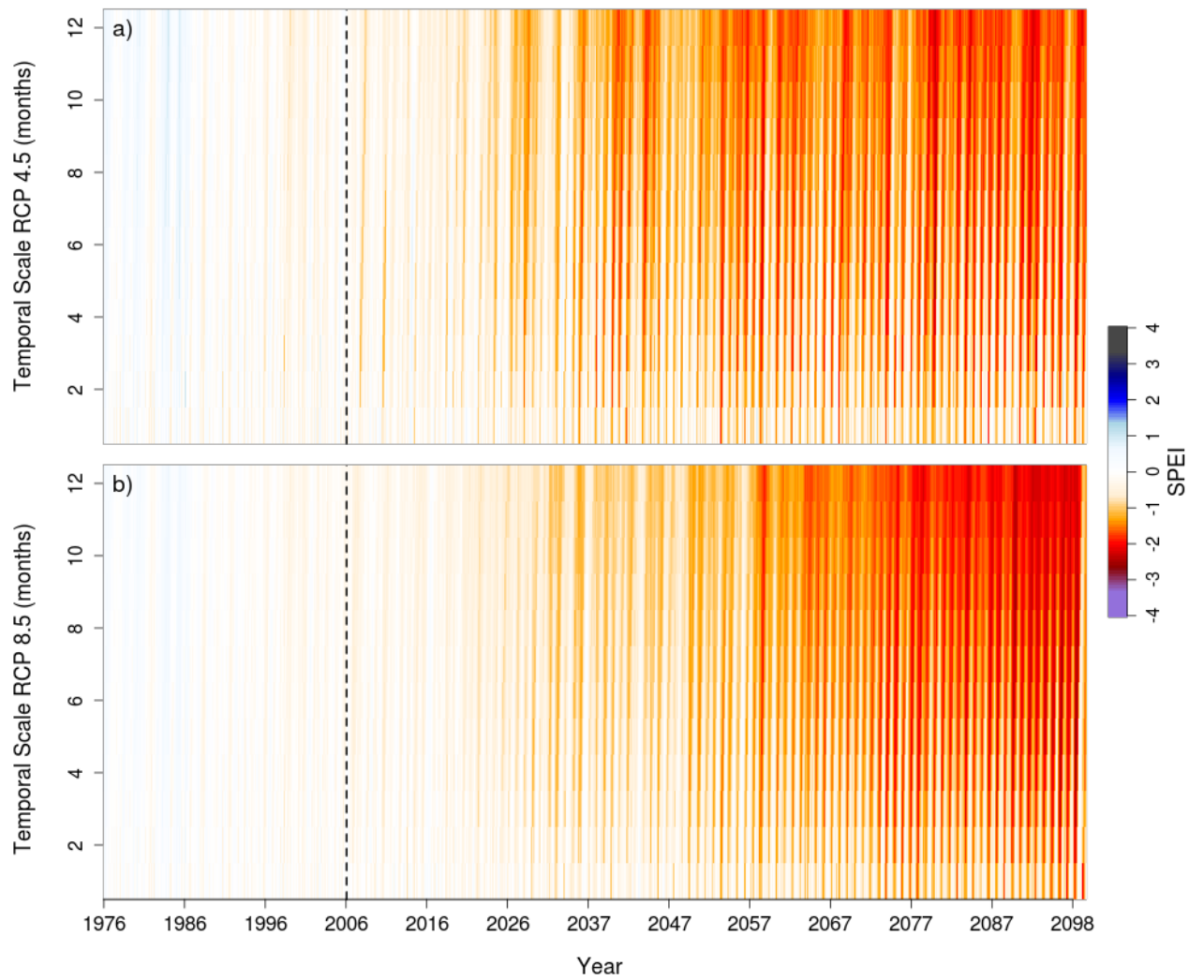


Figure 6. SPEI Time series under RCP4.5 and RCP8.5 along the 21st century at time-scales from 1 to 12 months. Data grouped for every RCP simulation of every global climate model and for every station. Both emissions scenarios are represented: RCP4.5 (figure a) and RCP8.5 (figure b)

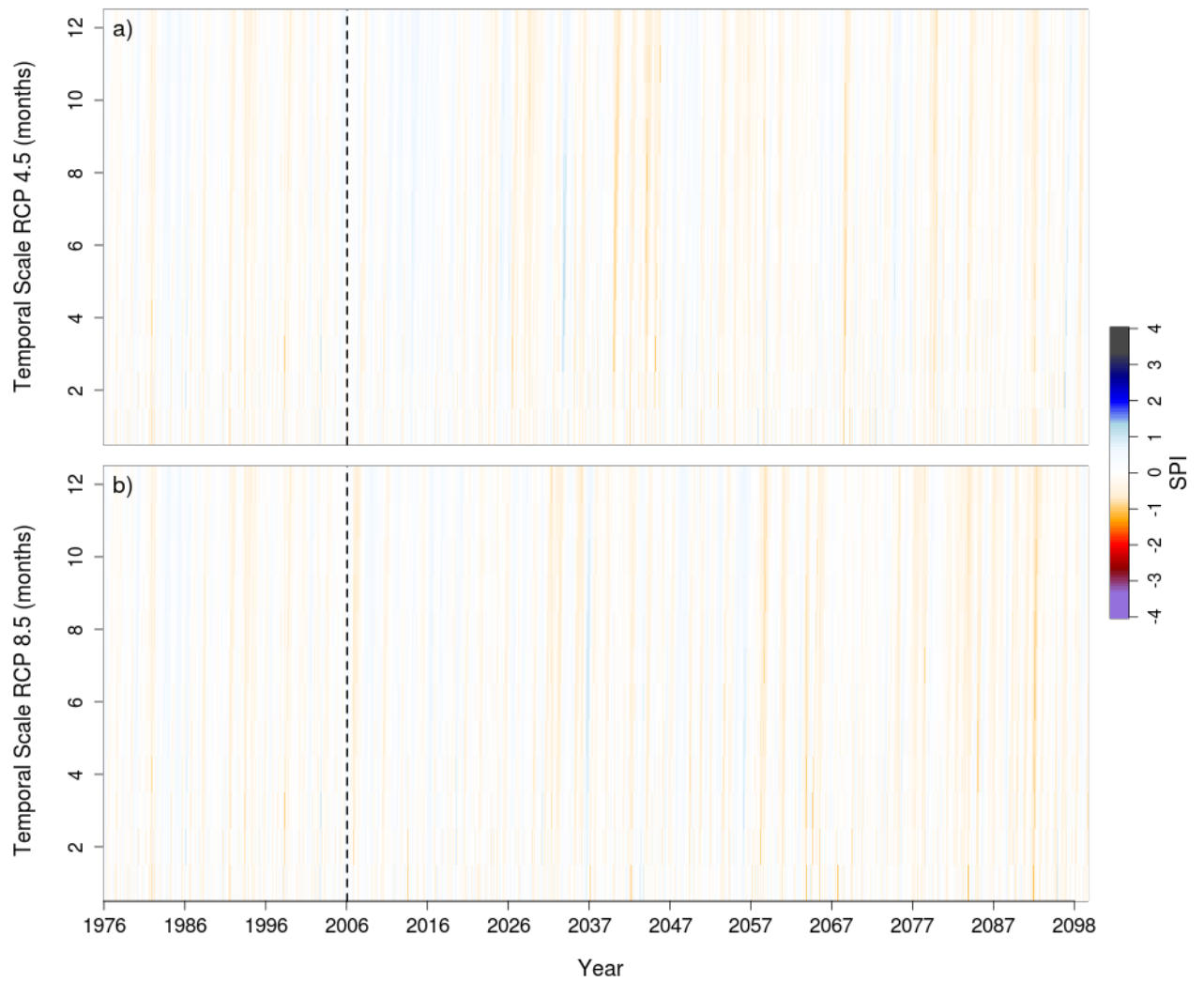


Figure 7. SPI Time series under RCP4.5 and RCP8.5 along the 21st century at time-scales from 1 to 12 months. Data grouped for every RCP simulation of every global climate model and for every station. Both emissions scenarios are represented: RCP4.5 (figure a) and RCP8.5 (figure b).

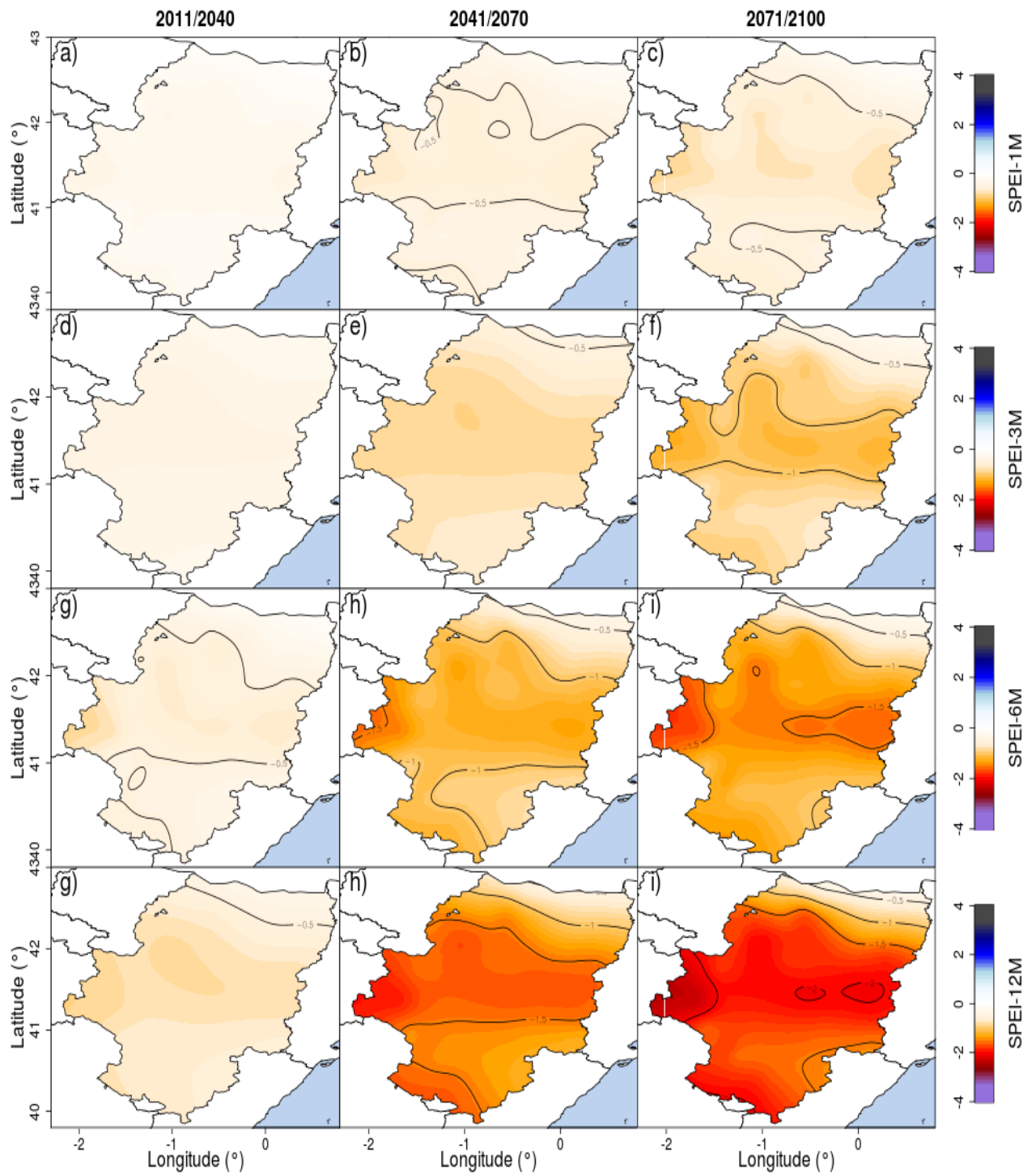


Figure 8. Time-scales SPEI maps under RCP4.5. Geographical representation of the expected evolution of the SPEI for Aragon in the periods 2041–2070 and 2071–2100 compared to the reference Historical Period (1971–2000) in terms of absolute values according to the RCP4.5 at different time-scales. The rows show the four time-scales analysed in the study (1 months, 3 months, 6 months and 12 months) and the columns, the three temporal periods (2011-2040, 2041–2070 and 2071–2100). The maps are generated by interpolating the available stations over the territory.

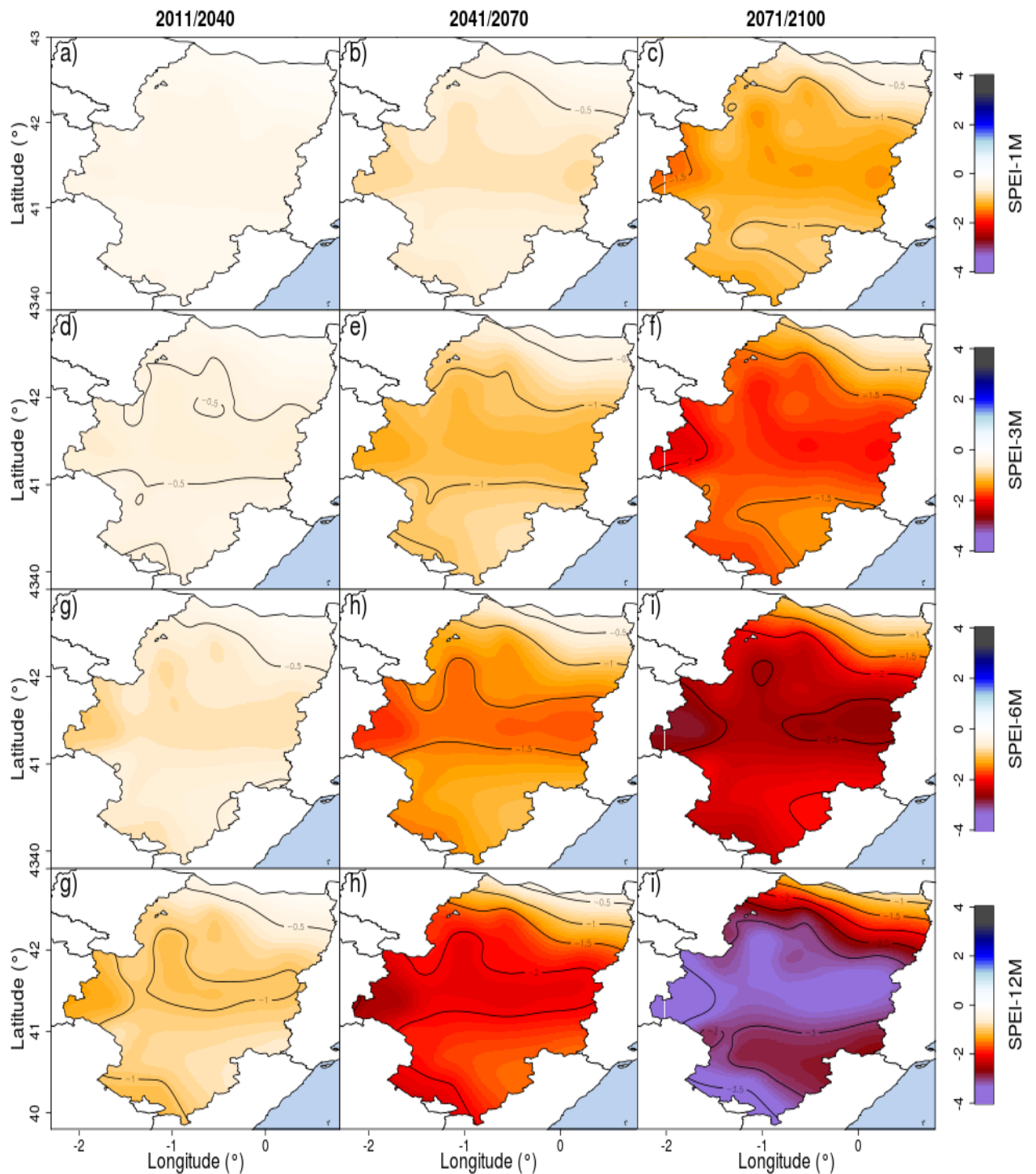


Figure 9. Time-scales SPEI maps under RCP8.5. Geographical representation of the expected evolution of the SPEI for Aragon in the periods 2041–2070 and 2071–2100 compared to the reference Historical Period (1971–2000) in terms of absolute values according to the RCP8.5 at different time-scales. The rows show the four time-scales analysed in the study (1 months, 3 months, 6 months and 12 months) and the columns the three temporal periods (2011–2040, 2041–2070 and 2071–2100). The maps are generated by interpolating the available stations over the territory.

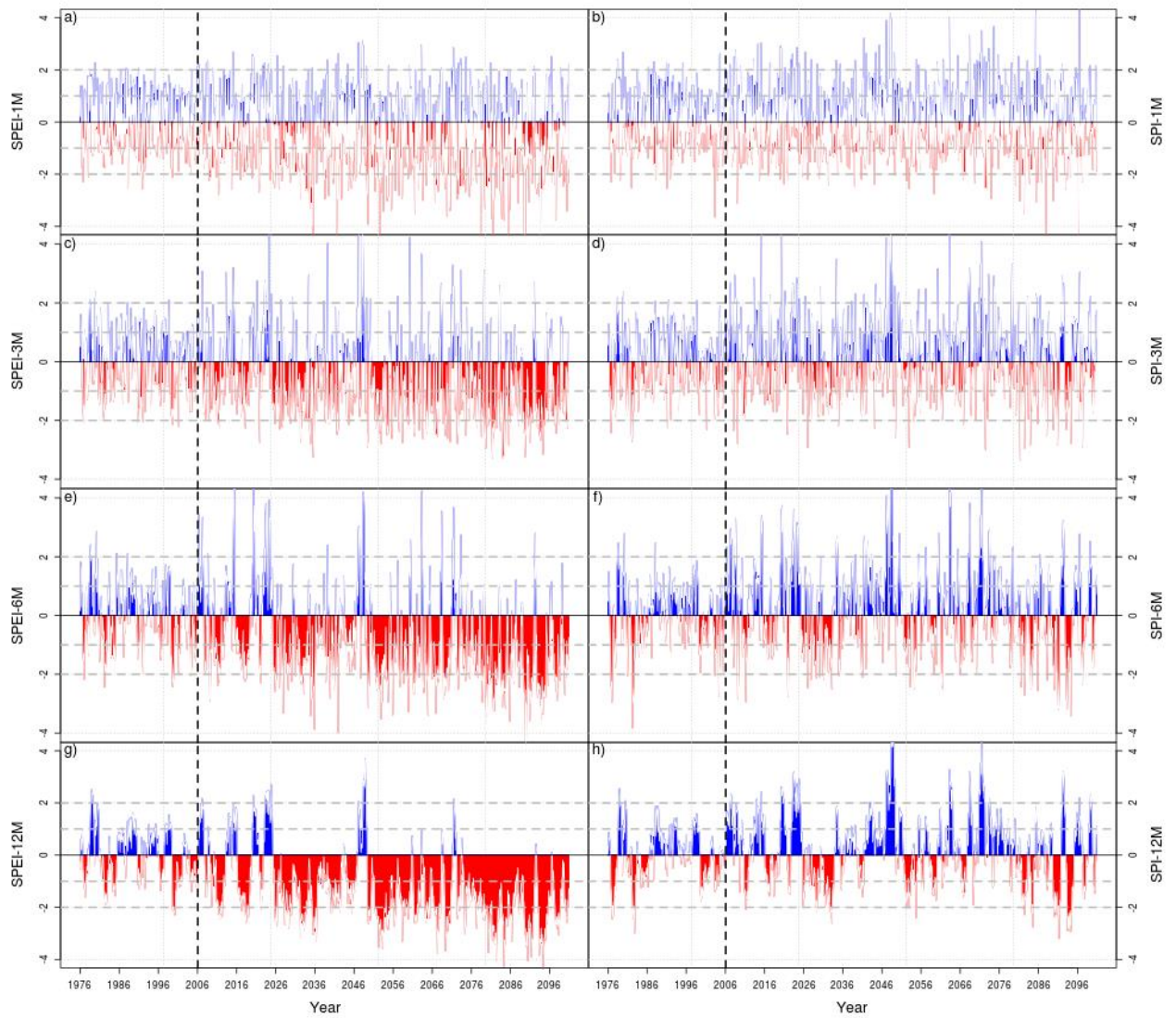


Figure 10. Time series for Zaragoza under MPI-ESM-MR RCP4.5. Evolution of the SPEI (first column) and the SPI (second column) based on the MPI-MR-SM model and under the RCP 4.5 at different time-scales - 1 month (first row), 3 months (second row), 6 months (third row) and 12 months (fourth row)- for Zaragoza.

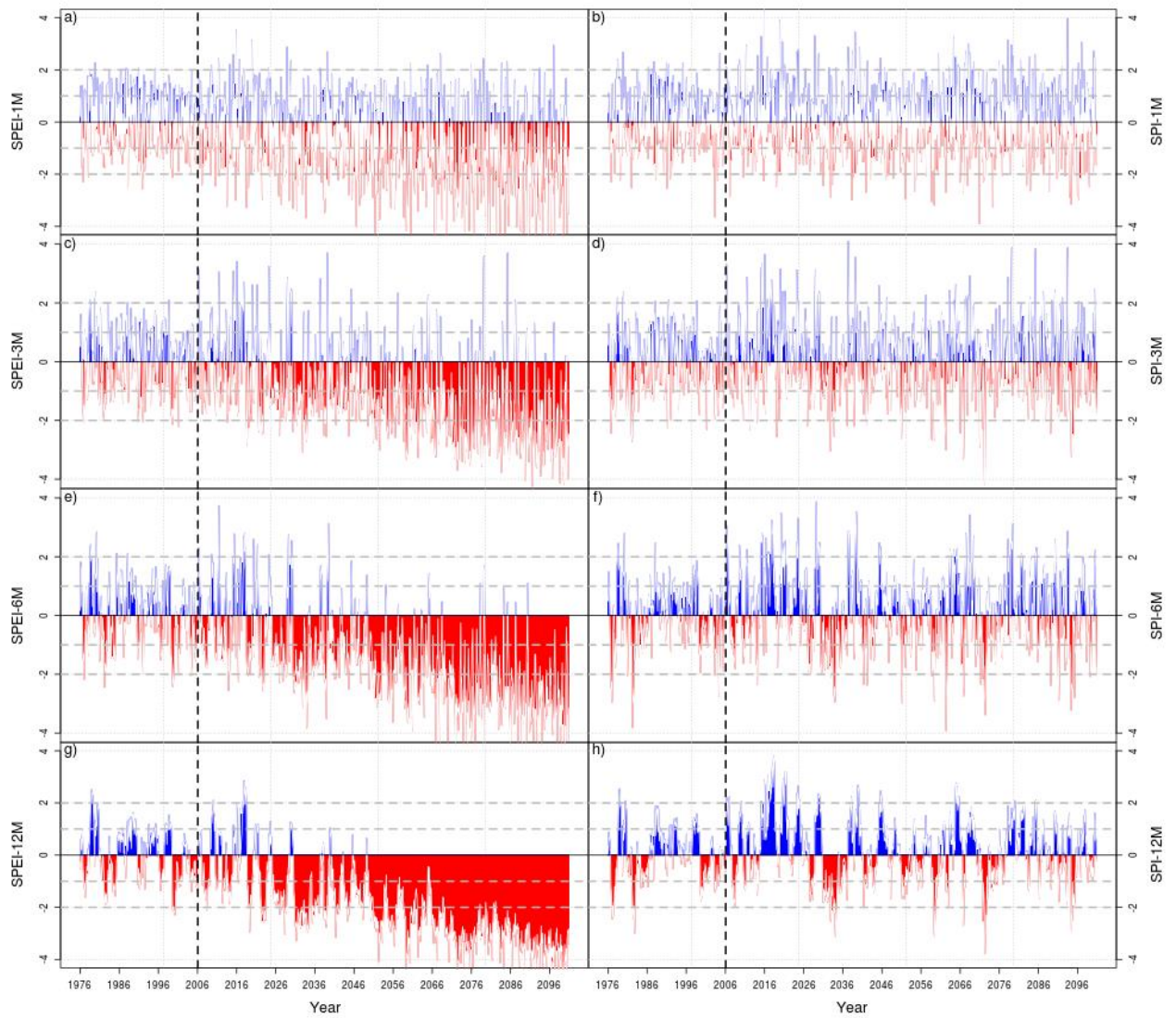


Figure. 11. Time series for Zaragoza under MPI-ESM-MR RCP8.5. Evolution of the SPEI (first column) and the SPI (second column) based on the MPI-MR-SM model and under the RCP 8.5 at different time-scales - 1 month (first row), 3 months (second row), 6 months (third row) and 12 months (fourth row)- for Zaragoza.

individual contributions, using the relevant CRediT roles:

Author	Individual contributions
Emma Gaitan	Data curation, Formal analysis, Investigation; Methodology, Software, Validation, Writing original draft, review and editing
Robert Monjo	Data curation, Methodology, Software, final review.
Javier Pórtoles	Data curation, Methodology, Software, final review
M ^a Rosa Pino-Otín	Formal analysis, Investigation; Methodology, Project administration, Supervision, Validation, Writing original draft, review and editing